Revisiting the Early Universe: A New Spectroscopic Analysis of $z \sim 6.4$ Quasar PSO J159-02

Christian Piscitelli, PhD Student @INAF OATs

Supervisors: Valentina d'Odorico, Stefano Borgani
Collaborators: Manuela Bischetti, Matilde Brazzini, Simona di Stefano

INAF OSSERVATORIO ASTRONOMICO DI TRIESTE
RECAP erc synergy grant
Funded by the European Union
UNIVERSITÀ DEGLI STUDI DI TRIESTE

Quasars: a brief introduction

Among the most luminous sources in the entire Universe

Capable to modify the surronding environment, including the host-galaxy itself

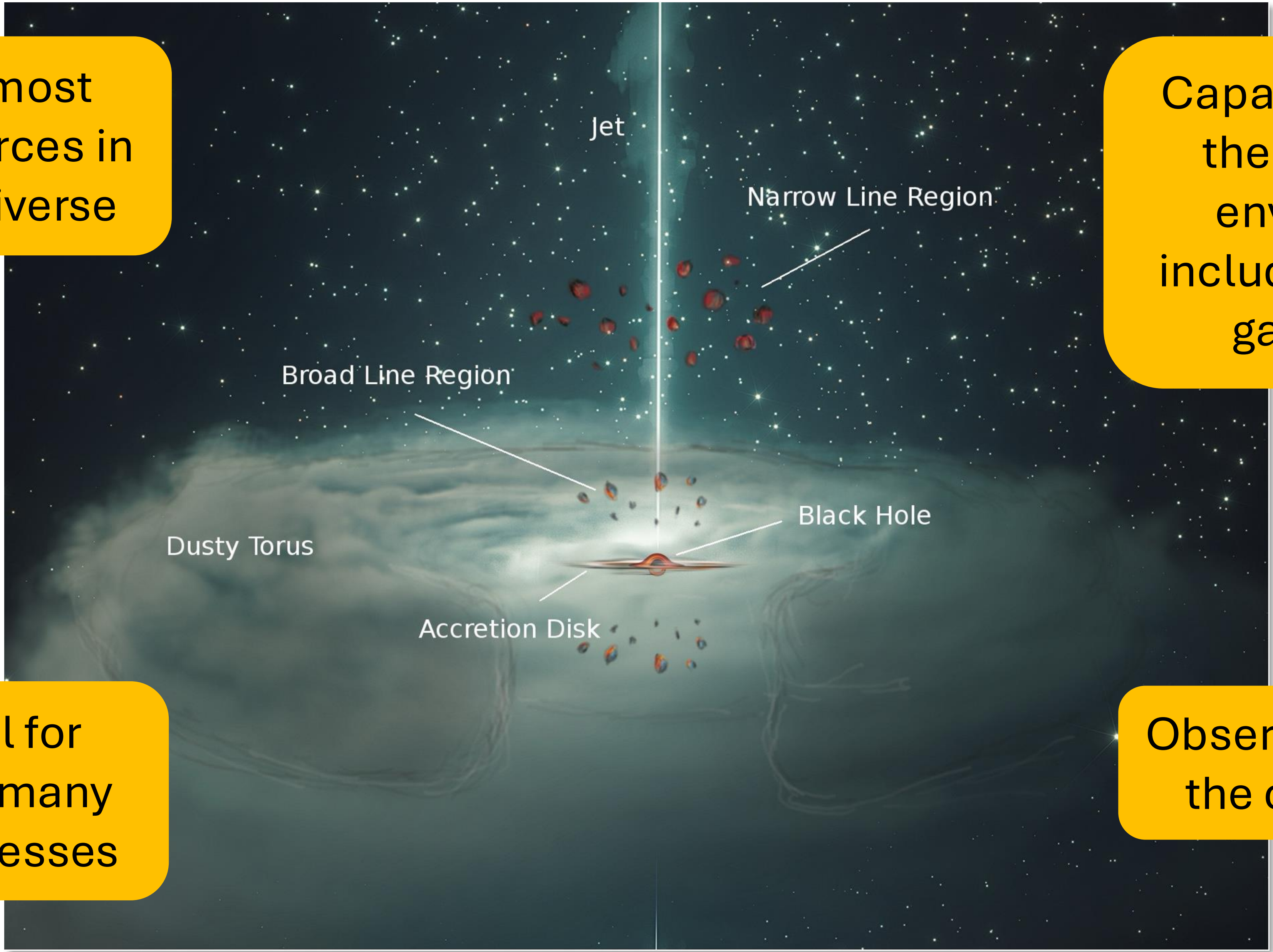

Optimal tool for investigating many physical processes

Observed across all the cosmic time

Quasars in the EoR

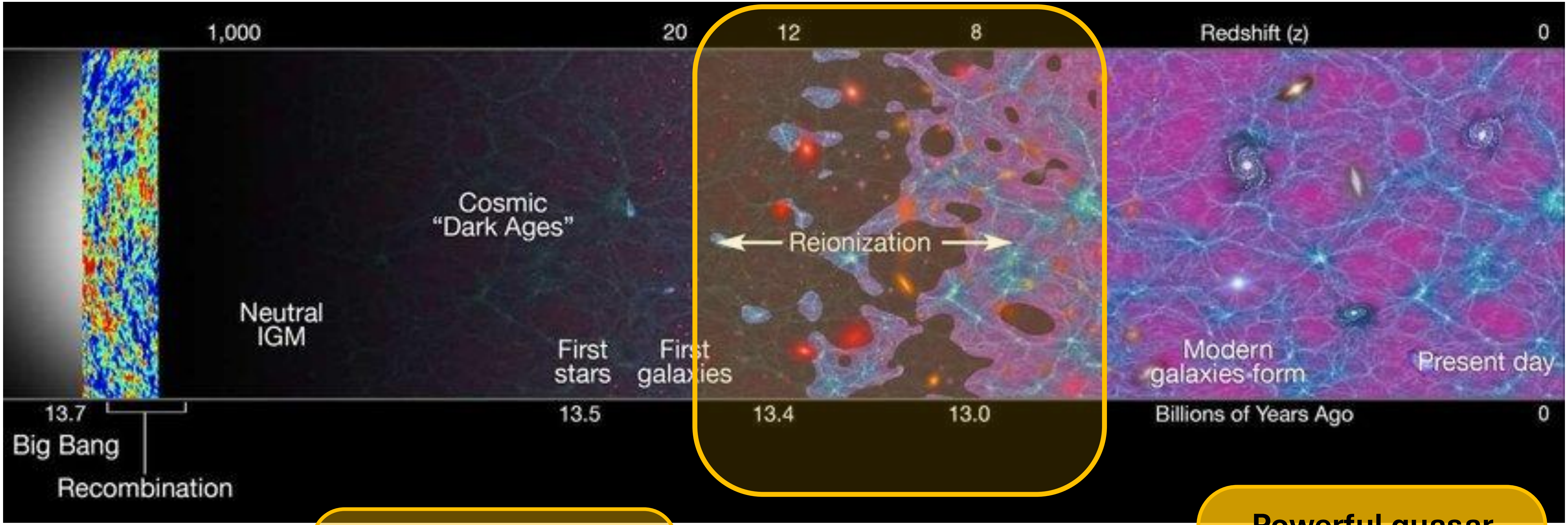

First astrophysical sources ionize the neutral Intergalactic Medium (IGM)

High-z quasars used as cosmic torches to probe IGM ionization

Powerful quasar outflows can enrich the surrounding IGM with heavy elements

Explore and investigate $z > 6$ quasars

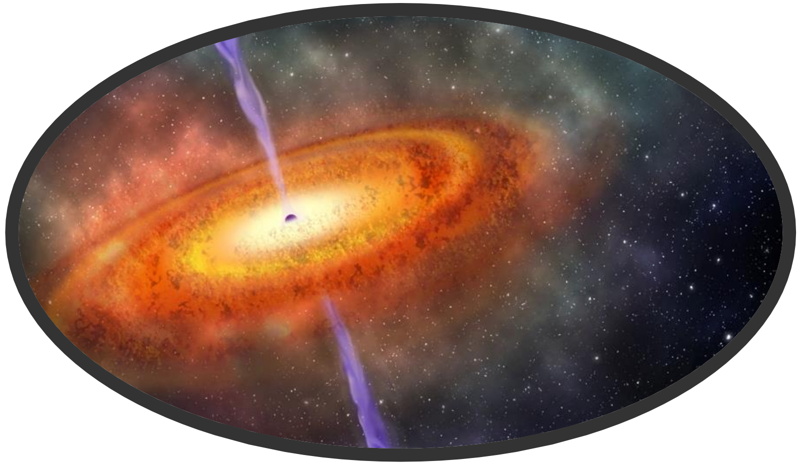

How do the first SMBH form and grow?
BH mass, Eddington luminosity ratio

How does feedback shape the SMBH-host galaxy evolution?
Stellar mass, Star Formation Rate

Explore and investigate $z > 6$ quasars

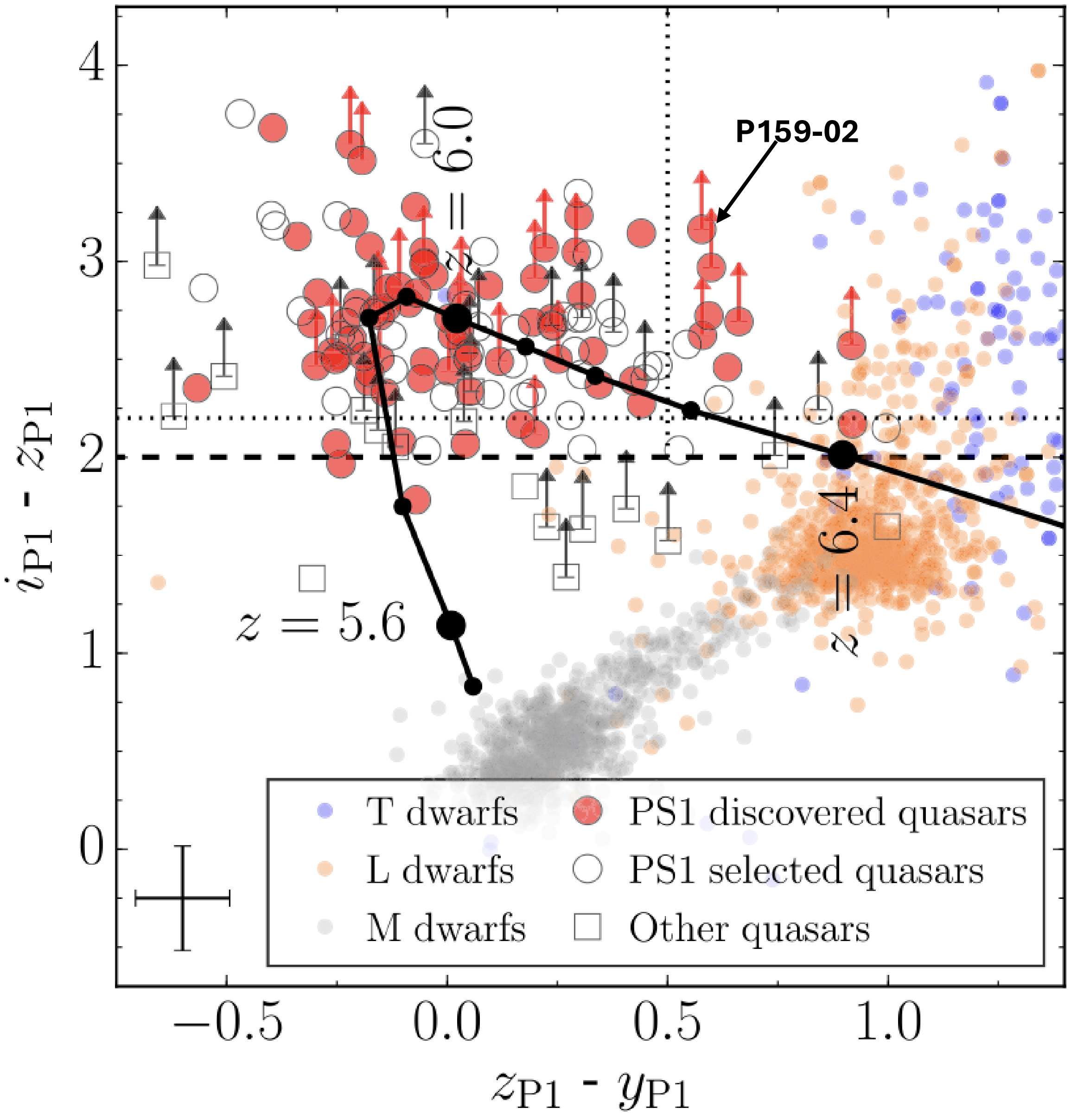

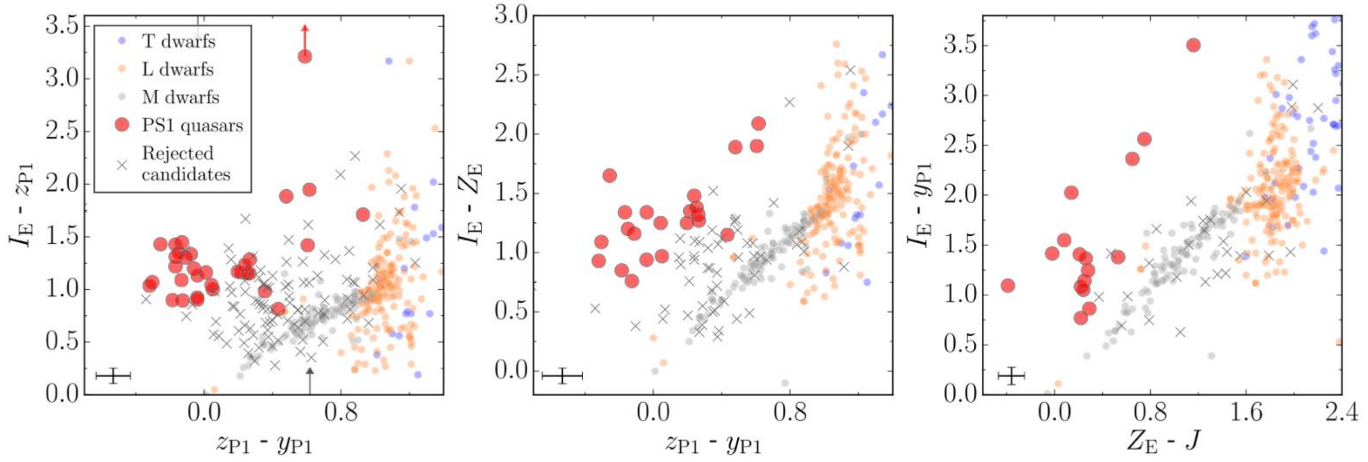

PSO J159-02 discoreved through photometric selection criteria and spectroscopically observed and confirmed with MMT/Red Channel

Bañados+ 2016

The quasar PSO J159-02

X-Ray *(XMM-Newton)*

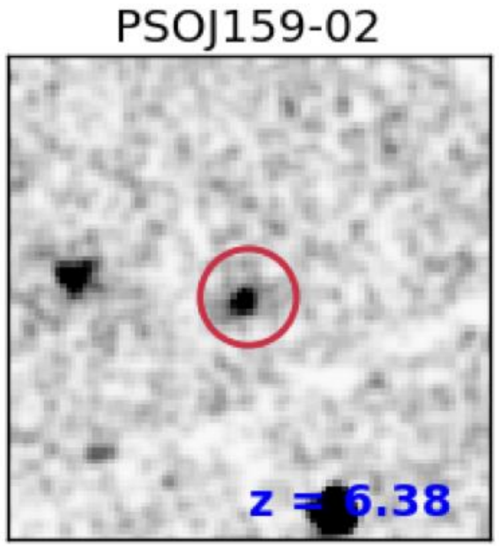

Energy range	Net counts	Flux (10^{-15} erg cm^{-2} s^{-1})	Det.
PSO J159.2257–02.5438 (z = 6.38)			
0.2 - 10 keV	127.1 ± 15.8	10.82 ± 1.35	8σ
0.2 - 0.5 keV	< 24.4	< 4.4	
0.5 - 2.0 keV	83.8 ± 11.8	4.11 ± 0.58	7σ
2.0 - 5.0 keV	26.5 ± 7.2	3.90 ± 1.13	4σ
5.0 - 10 keV	< 8.4	< 26.72	

Far Infrared: [C II] line

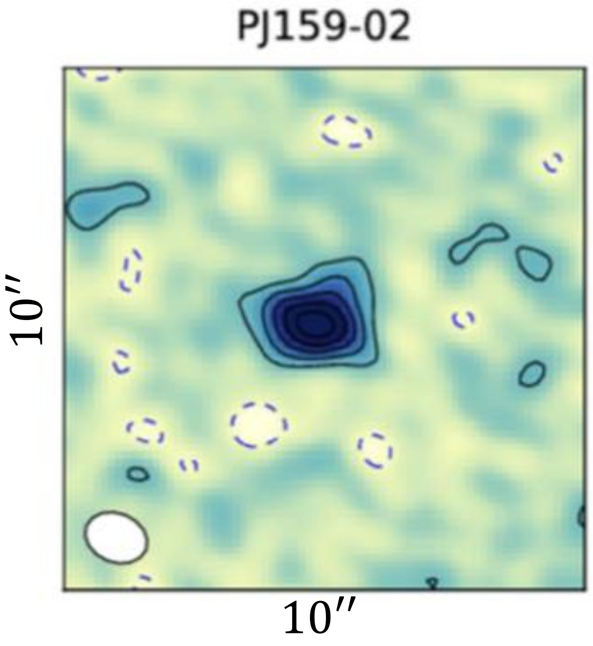

The solid black/dashed blue contours mark the $\pm 2, 4, 6, ..\sigma$ isophotes.

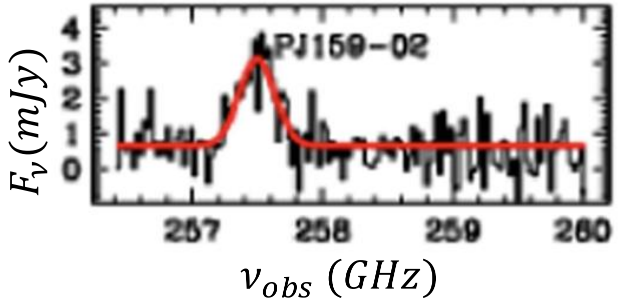

$$FWHM_{obs}([C\ II]) = 373^{+40}_{-39}\,\frac{km}{s}$$

$$z_{[C\ II]} = 6.3809 \pm 0.0005$$

Decarli+ 2018, Pons+ 2019

The quasar PSO J159-02

In more recent years, some studies have been conducted on samples of high-z quasars using VLT/X-Shooter spectrograph. Among them, PSO J159-02.

X-Shooter spectrograph is composed by:

- ~~UVB arm [300 – 550] nm~~
- VIS arm [550 – 1020] nm
- NIR arm [994 – 2480] nm

Although the quasar PSO J159-02 **has been recently investigated** using **VLT/X-Shooter** spectrograph, **only** the **NIR arm** has been used for the analysis.

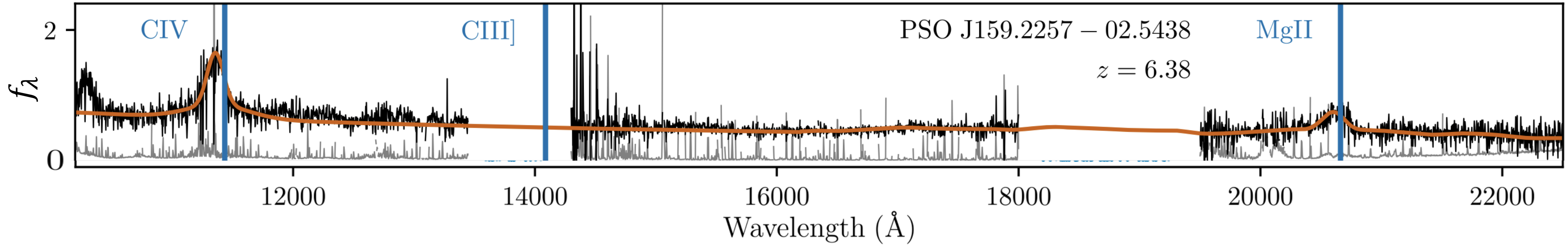

Schindler+ 2020, Farina+ 2022

The quasar PSO J159-02

We analyze observations conducted with **VLT/X-Shooter** spectrograph (**Programme/Run ID**: 0114.B-0278(A), **PI**: Luca Zappacosta) using both **VIS** and **NIR arms**.

The observations span a period from 25 January to 5 February 2025, totalling 24 observations.

PSO J159-02 observation: 04 February

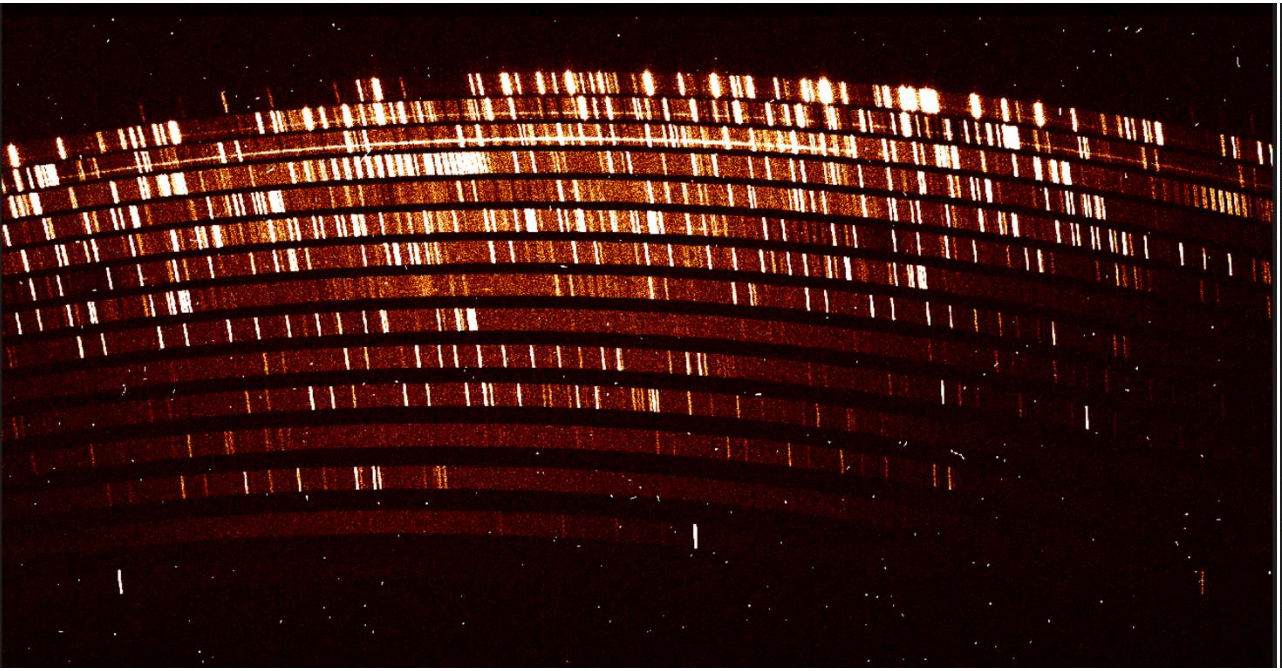

2-D spectrum: VIS

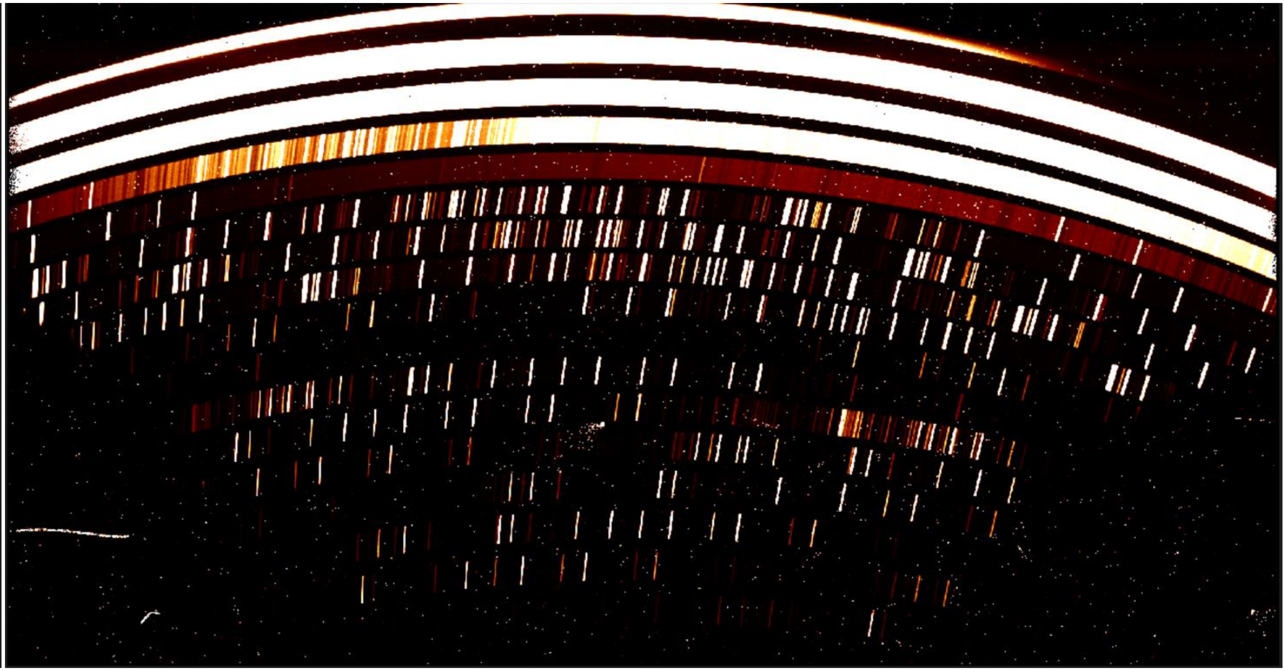

2-D spectrum: NIR

- In addition to this set, **we add 4 observations** dated **April** and **December 2017**.

Data reduction

For the **spectroscopic data reduction,** we used ***PypeIt*** (Prochaska et al. 2020). The main steps consist of:

- Basic image processing (i.e. flat-fielding)

- **Wavelength** (in vacuum) **solutions** for individual frames were derived
  - From **Th/Ar arc lamp** emission lines for the **VIS part**
  - From the **night sky** emission lines for the **NIR part**

- **Sky subtractions** were performed on the 2-D images by including both **image differencing** and a **B-spline fitting procedure**
  - For the **NIR** part of the spectrum an **ABBA dithering strategy** was adopted to subtract the bright and variable NIR sky background by differencing consecutive exposures

- **1-D spectrum** obtained from **optimal extraction** technique (Horne 1986)

- **Flux-calibration** of the individual 1-D spectrum **with the sensitivity function** derived from the standard star (GD 71) related to night observation

- **1D spectra coadding** and **stacking** of **multiple exposures**
  - Coadding routine construct wavelength grid which can be uniform in velocity. It has been chosen a dispersion of 10 km/s

- Fitting a **telluric absorption model** directly to the stacked quasar spectra **using** the telluric model grids produced from the Line-By-Line Radiative Transfer Model (***LBLRTM***: Clough et al. 2005)

VIS arm - 1D spectrum

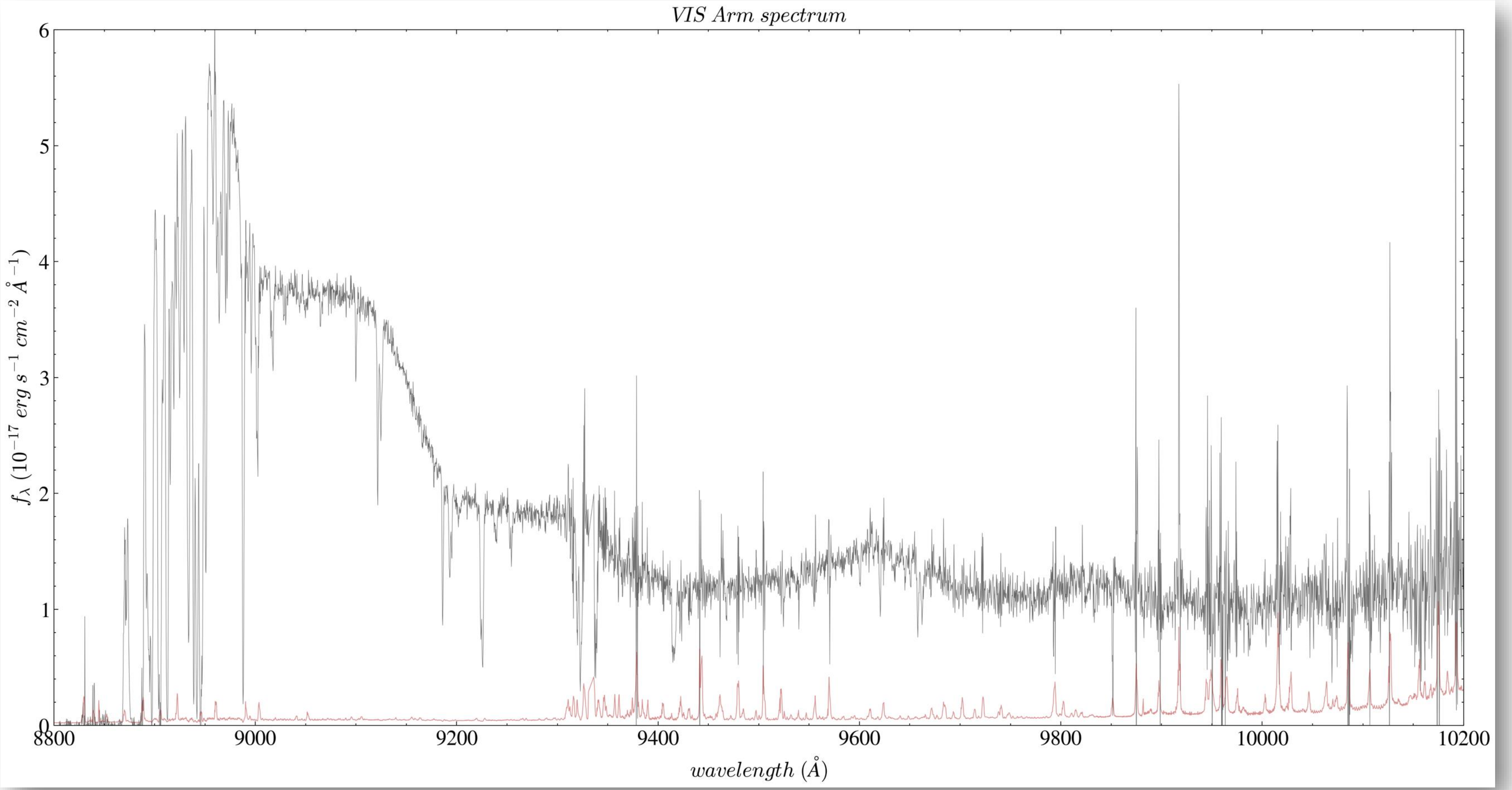

NIR arm - 1D spectrum

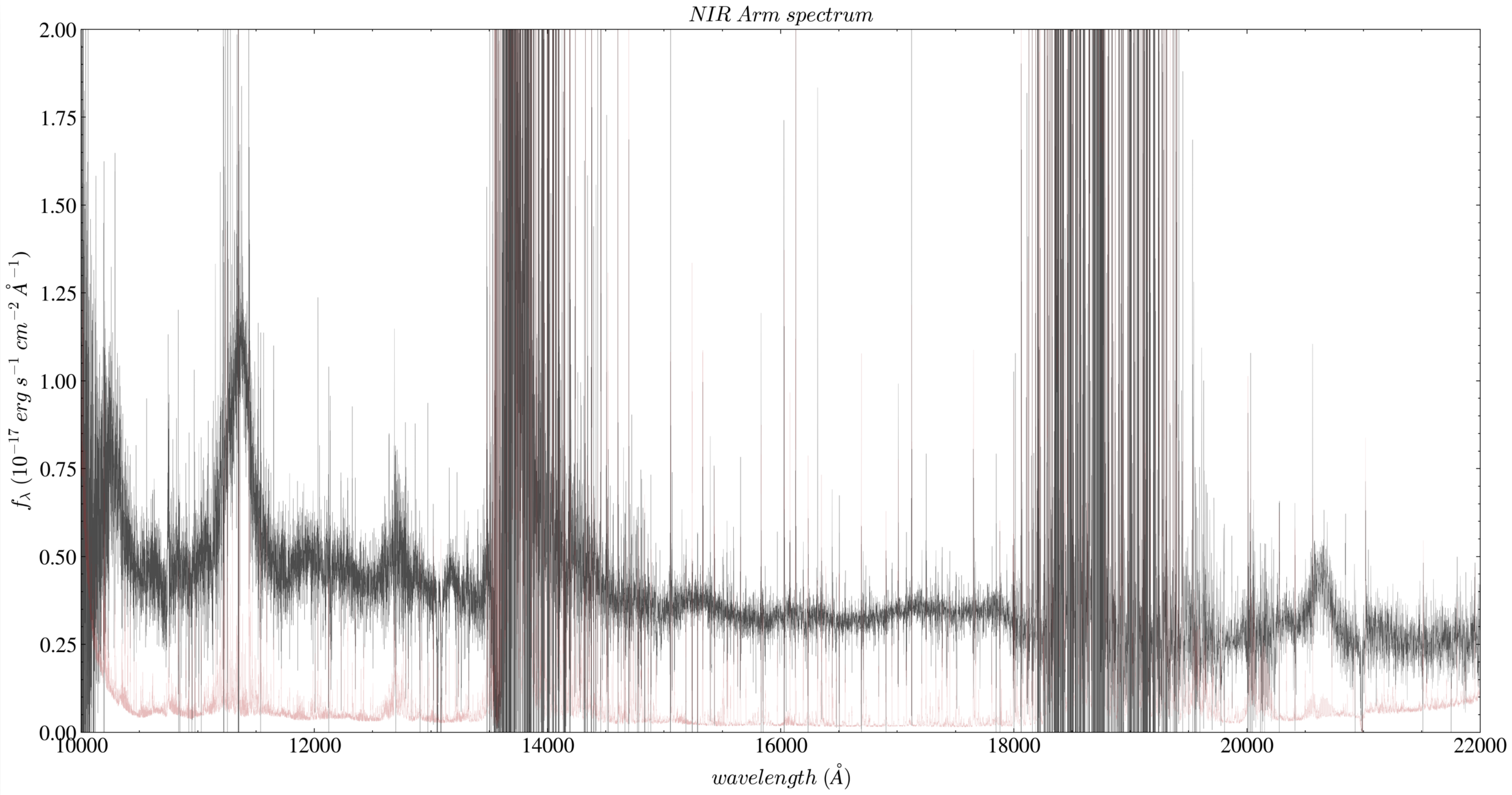

PSO J159-02 full 1D spectrum

- The NIR arm spectrum was scaled to the VIS one using the median values computed in the overlapping spectral region $1.00 - 1.02\ \mu m$
- The red end of the VIS arm spectrum and the blue end of the NIR arm were trimmed at $\lambda = 1.017\ \mu m$ to eliminate the noisiest regions

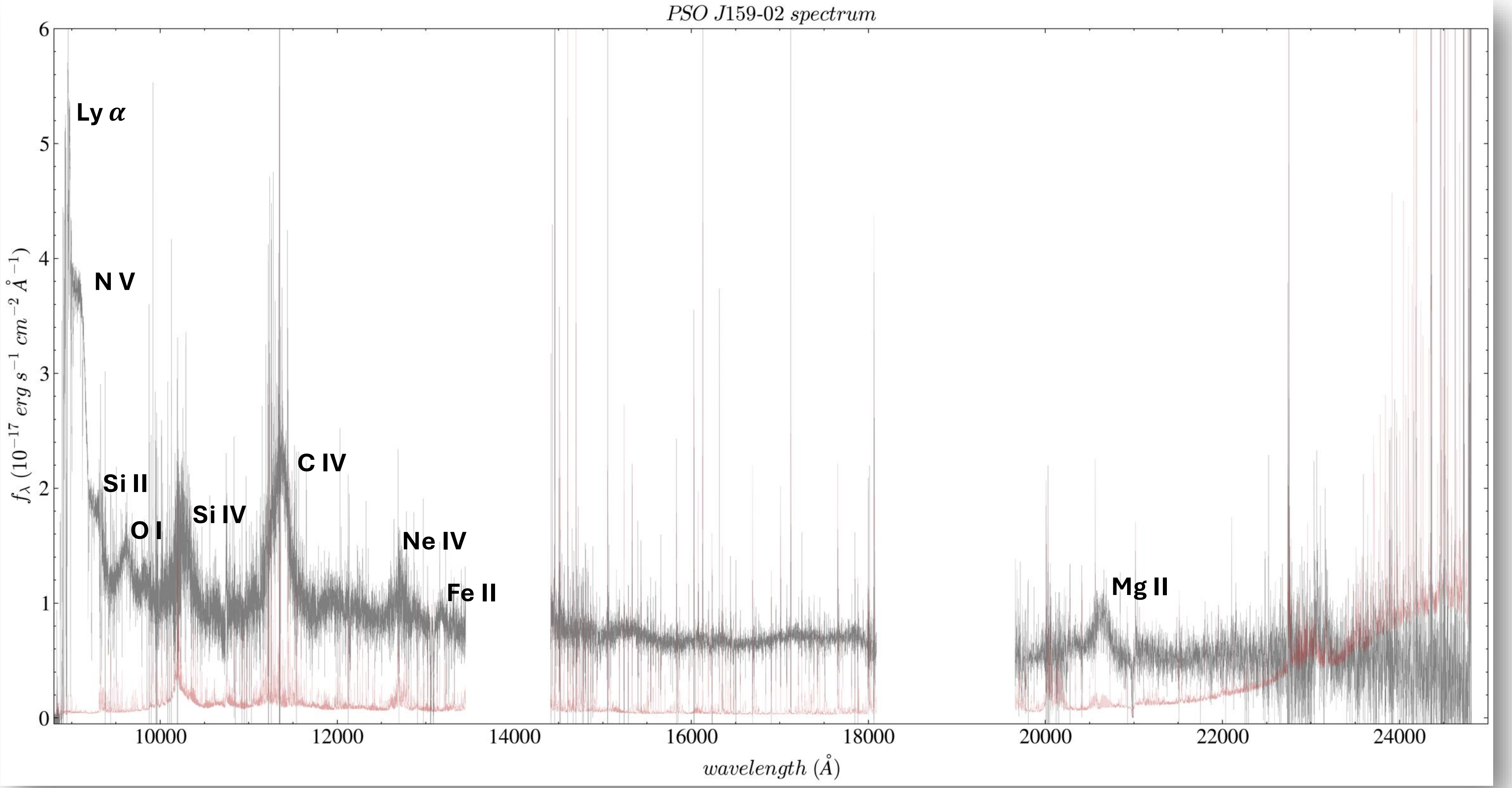

Rest-frame UV properties - Continuum

Assuming $\boldsymbol{z_{[C\,II]} = 6.38}$ as systemic redshift, we **modeled the continuum** as a **power-law** plus **Balmer continuum** (Dietrich et al. 2003):

- Power-law: $f_{PL}(\lambda) = f_{PL,0}\left(\frac{\lambda}{2500\ \text{Å}}\right)^{-\alpha_\lambda}$
- Balmer pseudo-continuum: $f_{BC}(\lambda) = f_{BC,0} B_\lambda(\lambda, T_e)\left(1 - e^{\left(-\tau_{BE}(\lambda/\lambda_{BE})^3\right)}\right)\ \forall\ \lambda \leq \lambda_{BE}$
- We **fix** the Balmer continuum **contribution to 30%** of the power-law (Onoue et al. 2020): $f_{BC}(3646\ \text{Å}, f_{BC,0}) = 0.3 \times f_{PL,0}(3646\ \text{Å})$

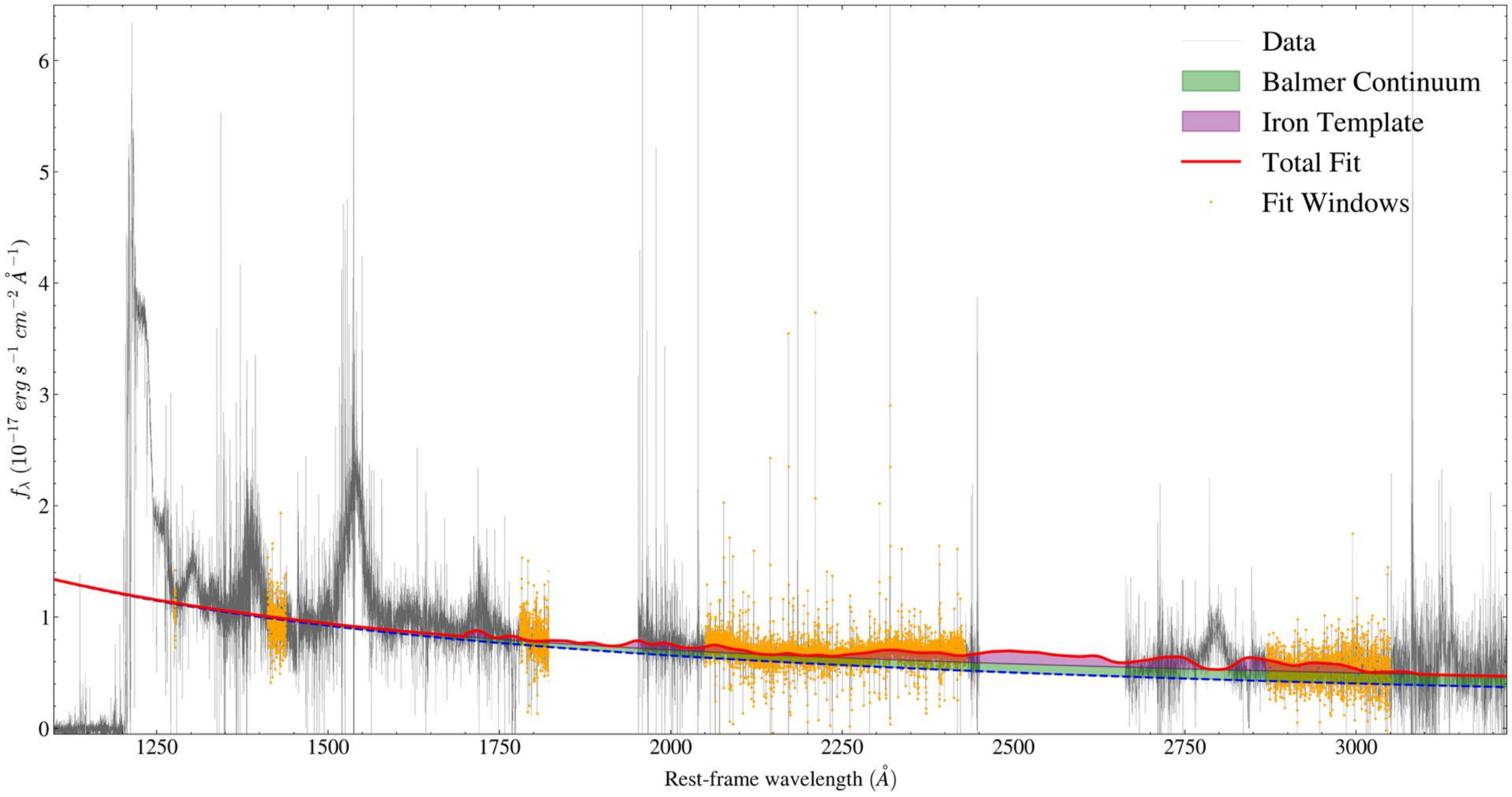

- In addition, we **include the iron pseudo-continuum** in the fit with a **template** derived from the **narrow-lne Seyfert 1 galaxy I Zwicky 1** (Vestergaard & Wilkes 2001)

Results from the continuum fit:

$\boldsymbol{\alpha_\lambda = -1.19 \pm 0.02}$

$\boldsymbol{f_{PL,0} = 0.502 \pm 0.004}$

Rest-frame UV properties – C IV emission line

We model the ***C IV emission*** line as **double gaussian component**, in the wavelengths window [1470, 1600] Å.

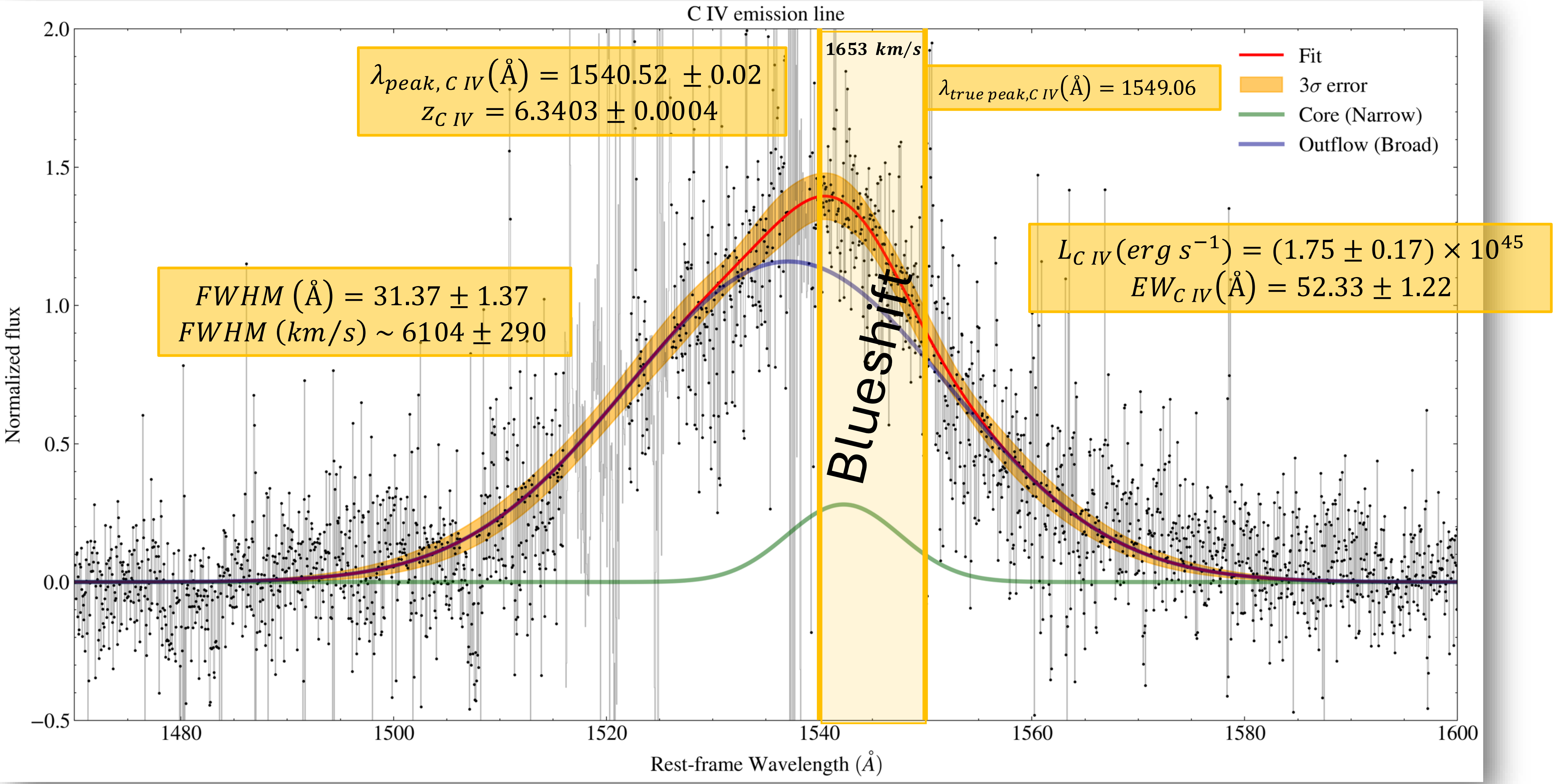

Rest-frame UV properties – Mg II emission line

We model the ***Mg II emission*** line as **single gaussian component**, in the wavelengths window [2700, 2900] Å.

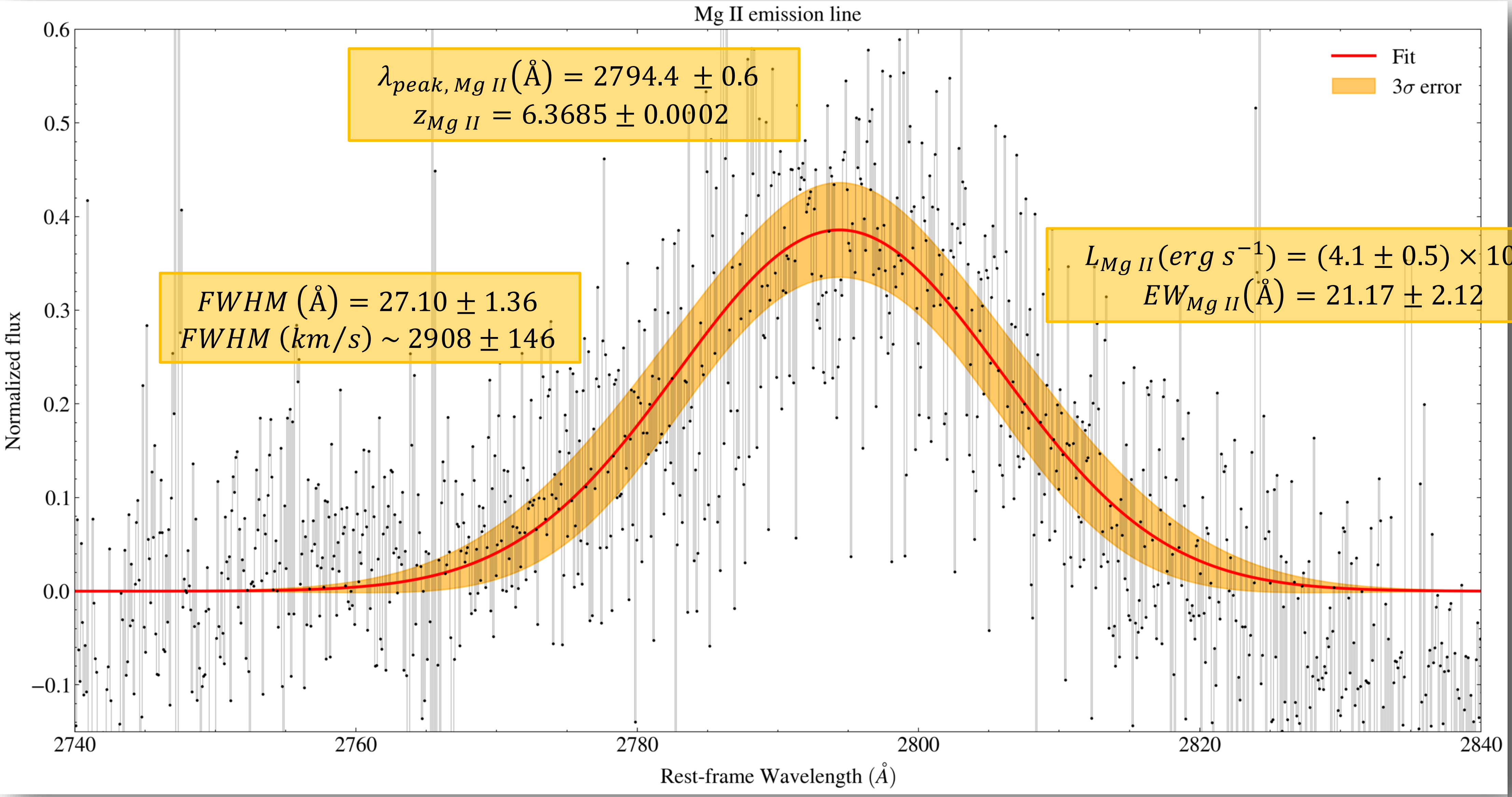

Rest-frame UV properties – Si IV emission line

We model the ***Si IV emission*** line as **single gaussian component,** in the wavelengths window [1360, 1430] Å.

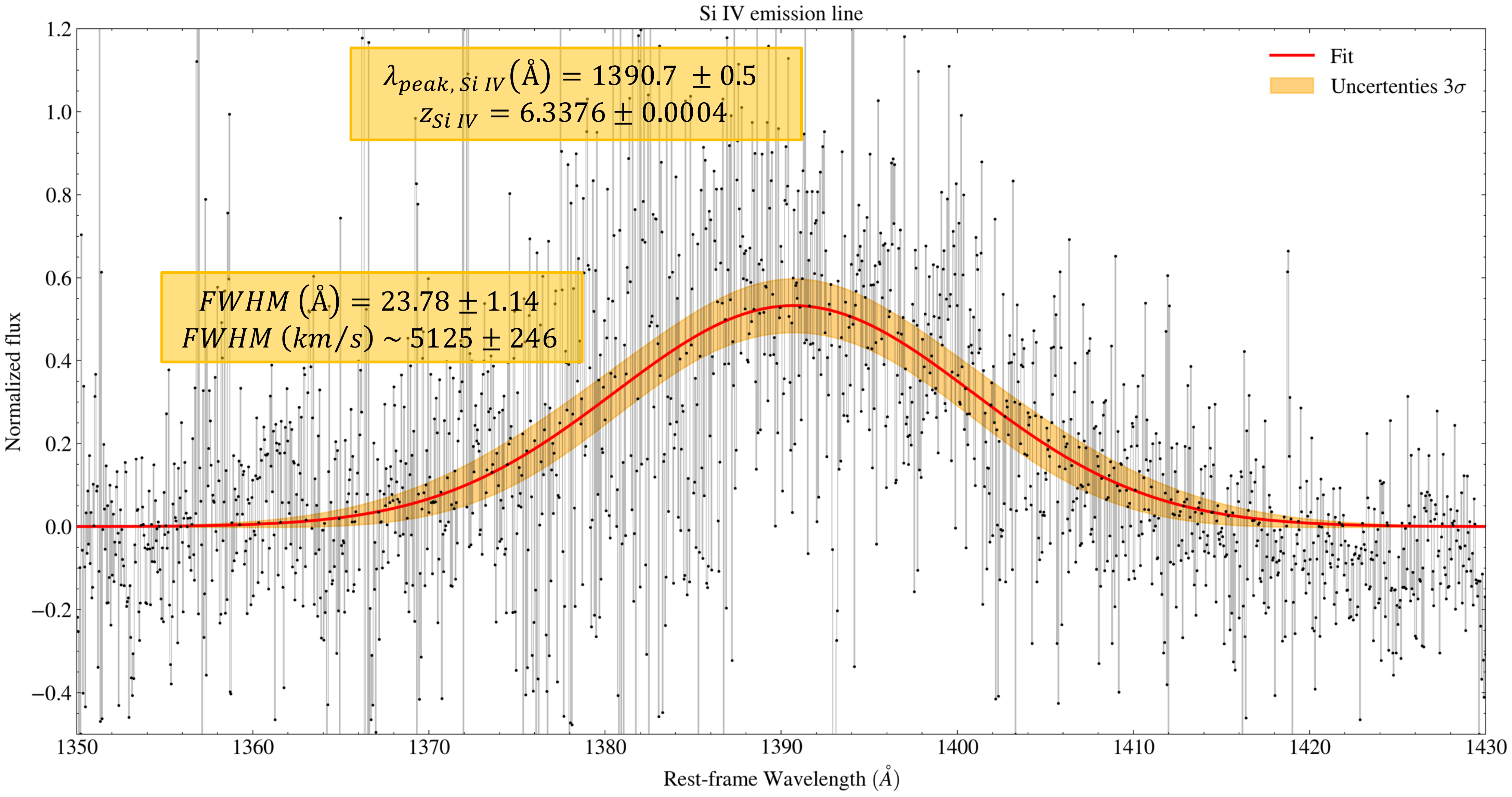

Rest-frame UV properties – Velocity Shift

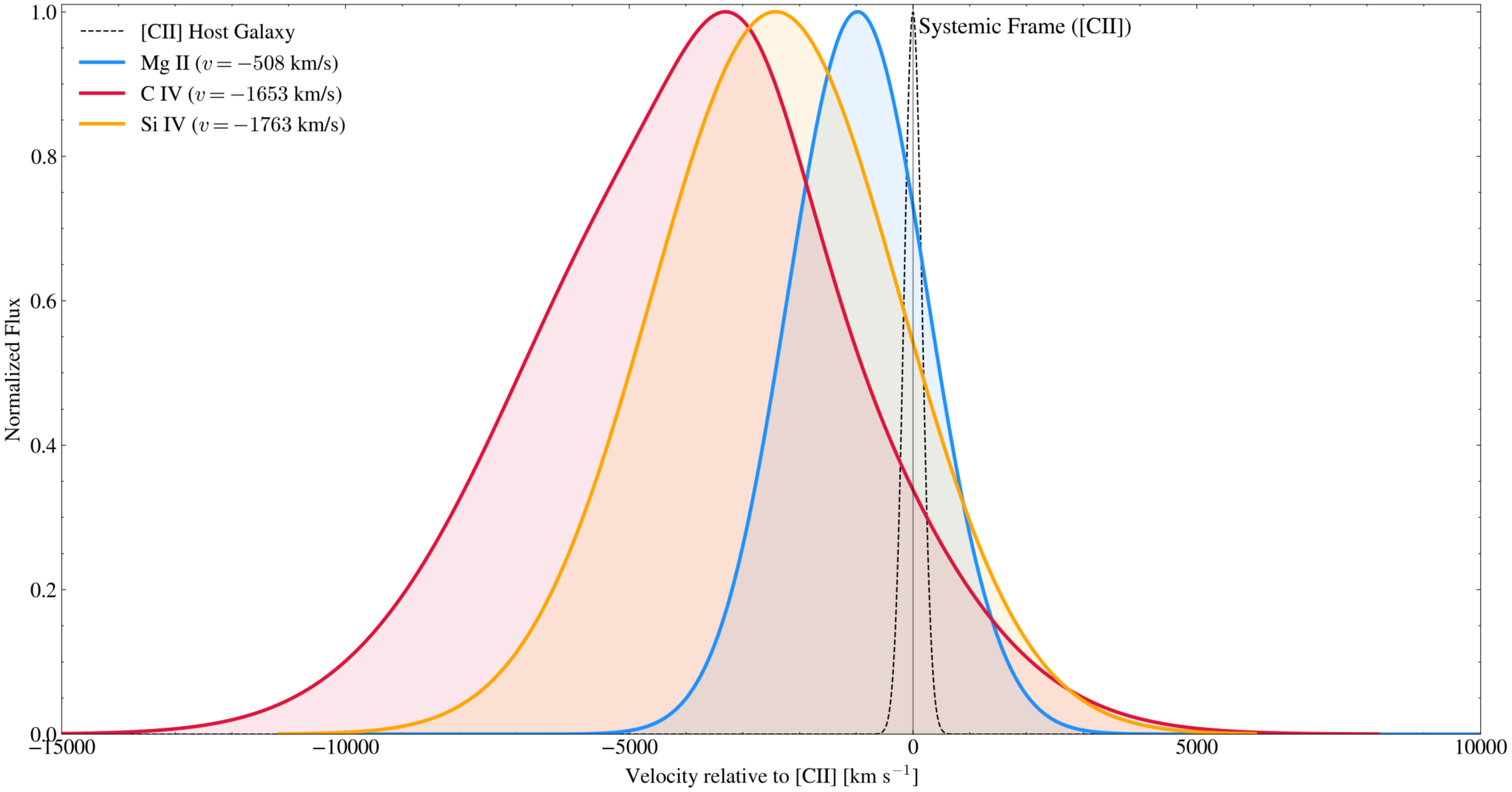

Rest-frame UV properties - BH mass and Eddington ratio

We derive the bolometric luminosity at 3000 Å (Richard+ 2006) obtaining

$$L_{bol} = 5.15 \times \lambda L_\lambda(3000\ \text{Å})\ erg/s = (3.01 \pm 0.03) \times 10^{47}\ erg/s$$

Mg II BH mass

We use the **scaling relation** from Vestergaard & Osmer (2009):

$$M_{\rm BH,MgII} = 10^{6.86} \left[\frac{FWHM_{\rm Mg\,II}}{10^3\ \rm km\,s^{-1}}\right]^2 \left[\frac{\lambda L_\lambda\,(3000\ \text{Å})}{10^{44}\ \rm erg\,s^{-1}}\right]^{0.5} M_\odot$$

$$\log\left(\frac{M_{BH,Mg\ II}}{M_\odot}\right) = 9.53 \pm 0.04$$

C IV BH mass

We use the **scaling relation** from Vestergaard & Peterson (2006):

$$M_{\rm BH,CIV} = 10^{6.66} \left[\frac{FWHM_{\rm C\,IV,corr}}{10^3\ \rm km\,s^{-1}}\right]^2 \left[\frac{\lambda L_\lambda\,(1350\ \text{Å})}{10^{44}\ \rm erg\,s^{-1}}\right]^{0.53} M_\odot$$

$$\log\left(\frac{M_{BH,C\ IV}}{M_\odot}\right) = 9.51 \pm 0.05$$

$$\lambda_{Edd,C\ IV} = 0.74 \pm 0.06$$
$$\lambda_{Edd,Mg\ II} = 0.71 \pm 0.05$$

Excellent agreement!

Rest-frame UV properties – comparison with literature

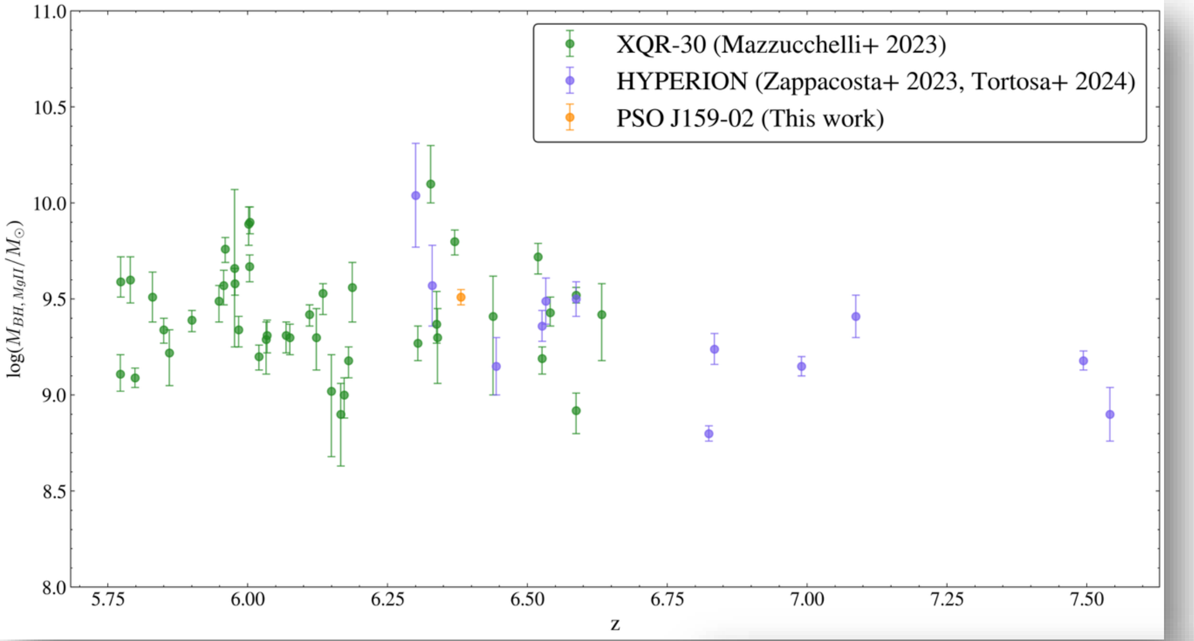

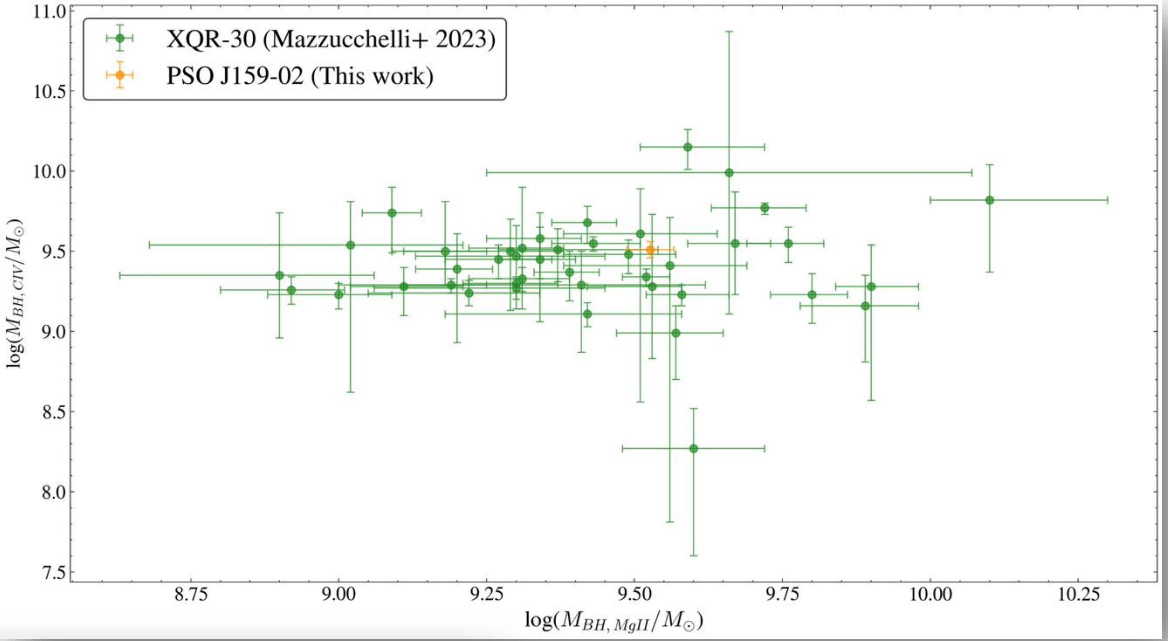

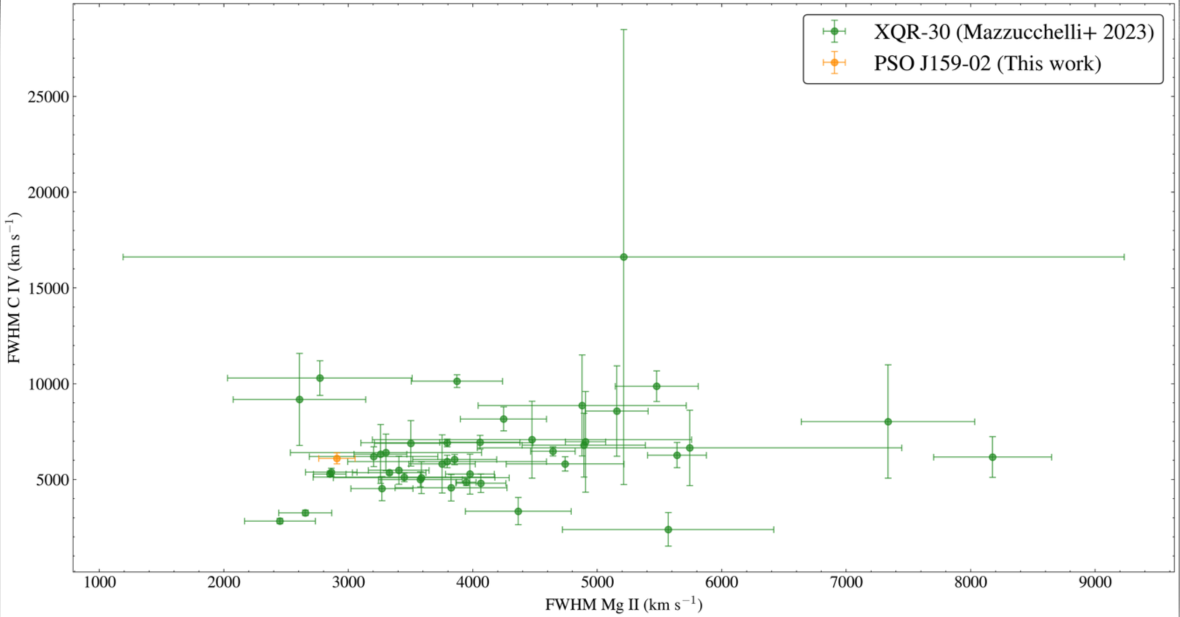

Rest-frame UV properties – comparison with literature

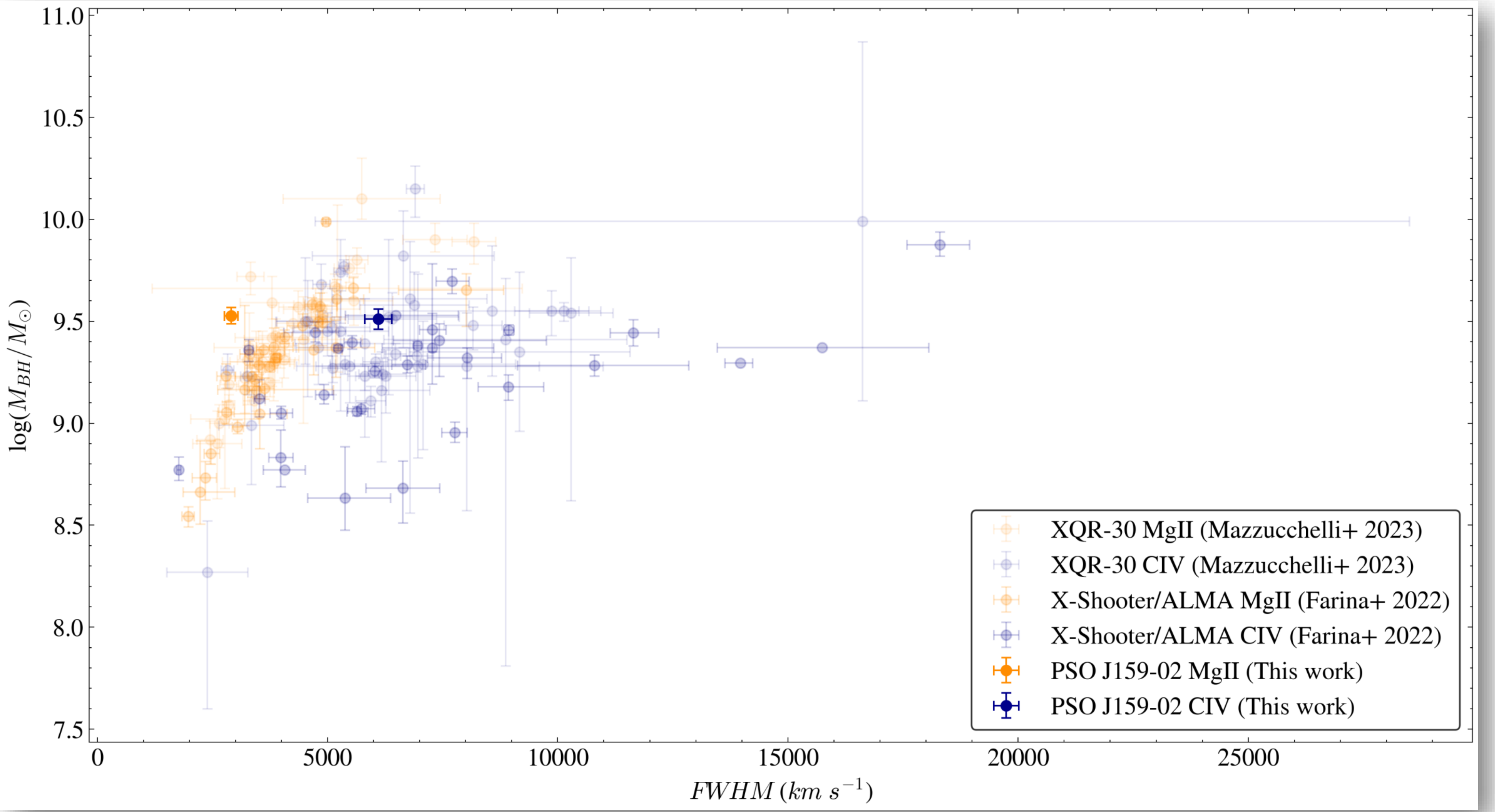

PSO J159-02 Field of View (EIGER)

JWST/NIRCam observations with F115W, F200W, and F356W

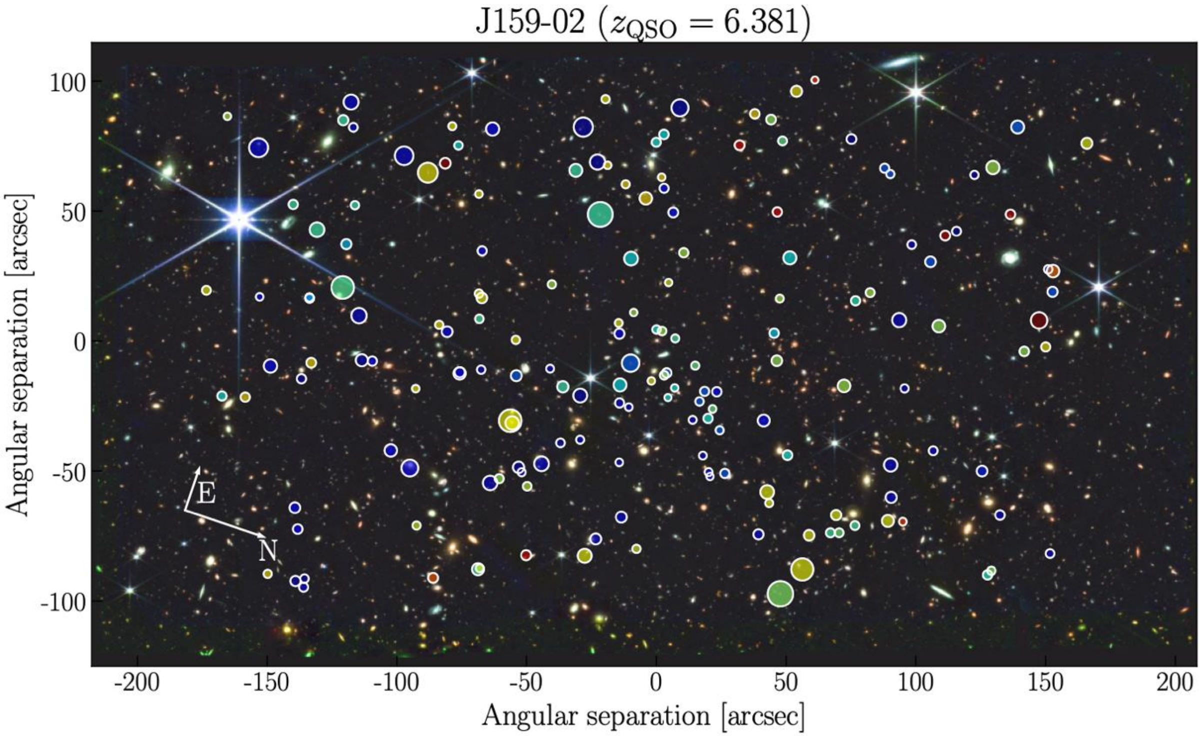

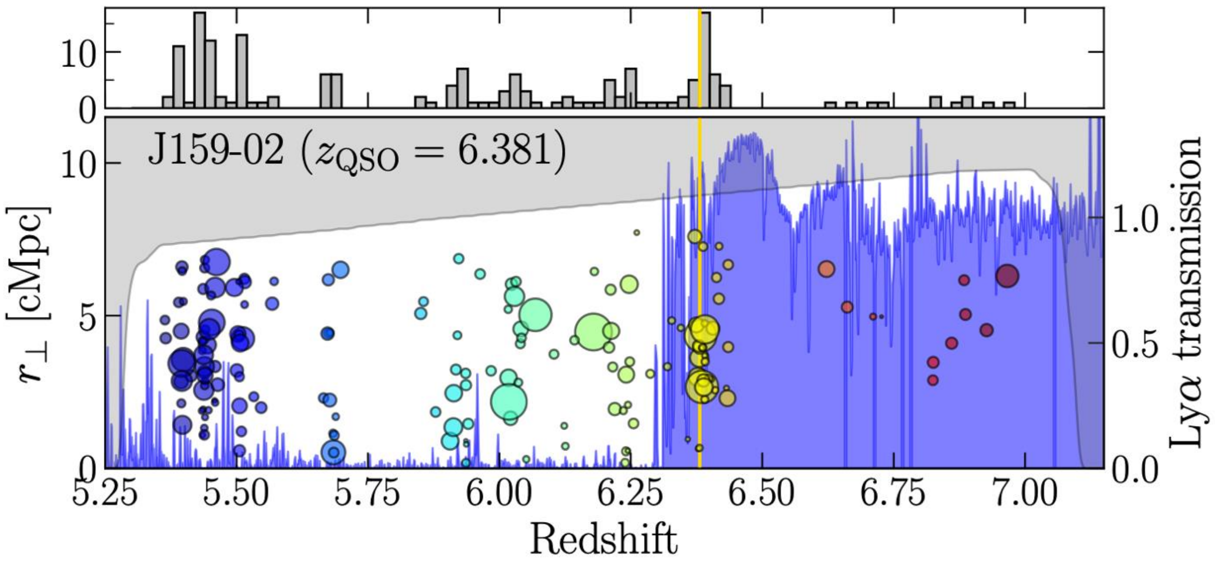

The circles are [O III] emitters, and the shape indicates their luminosity

Kashino+ 2025

Intervening absorbers in J159-02 spectrum

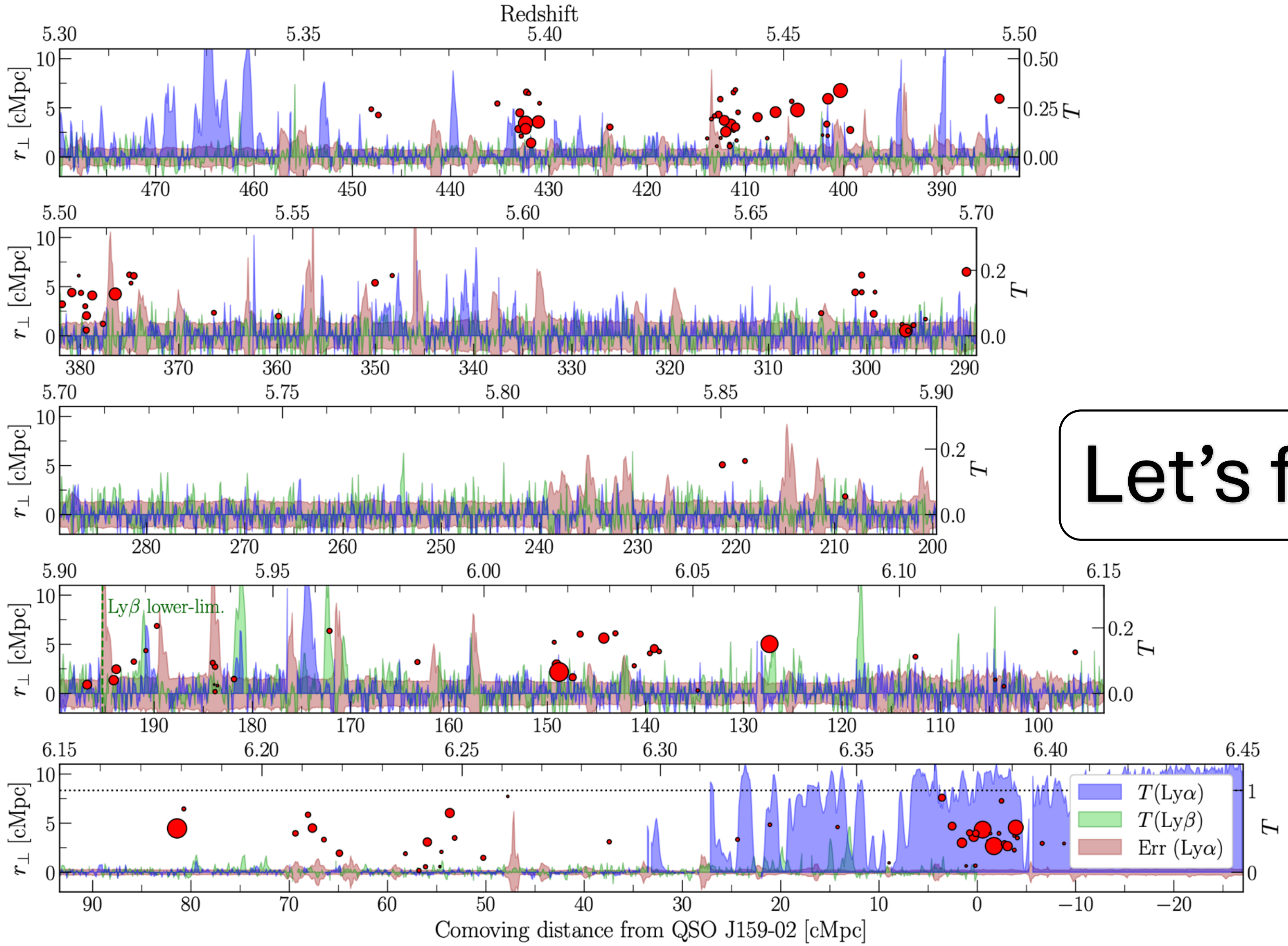

Let's find the absorbers!

Kashino+ 2025

Intervening absorbers in J159-02 spectrum (1)

Absorption system at $z \sim 5.91309$

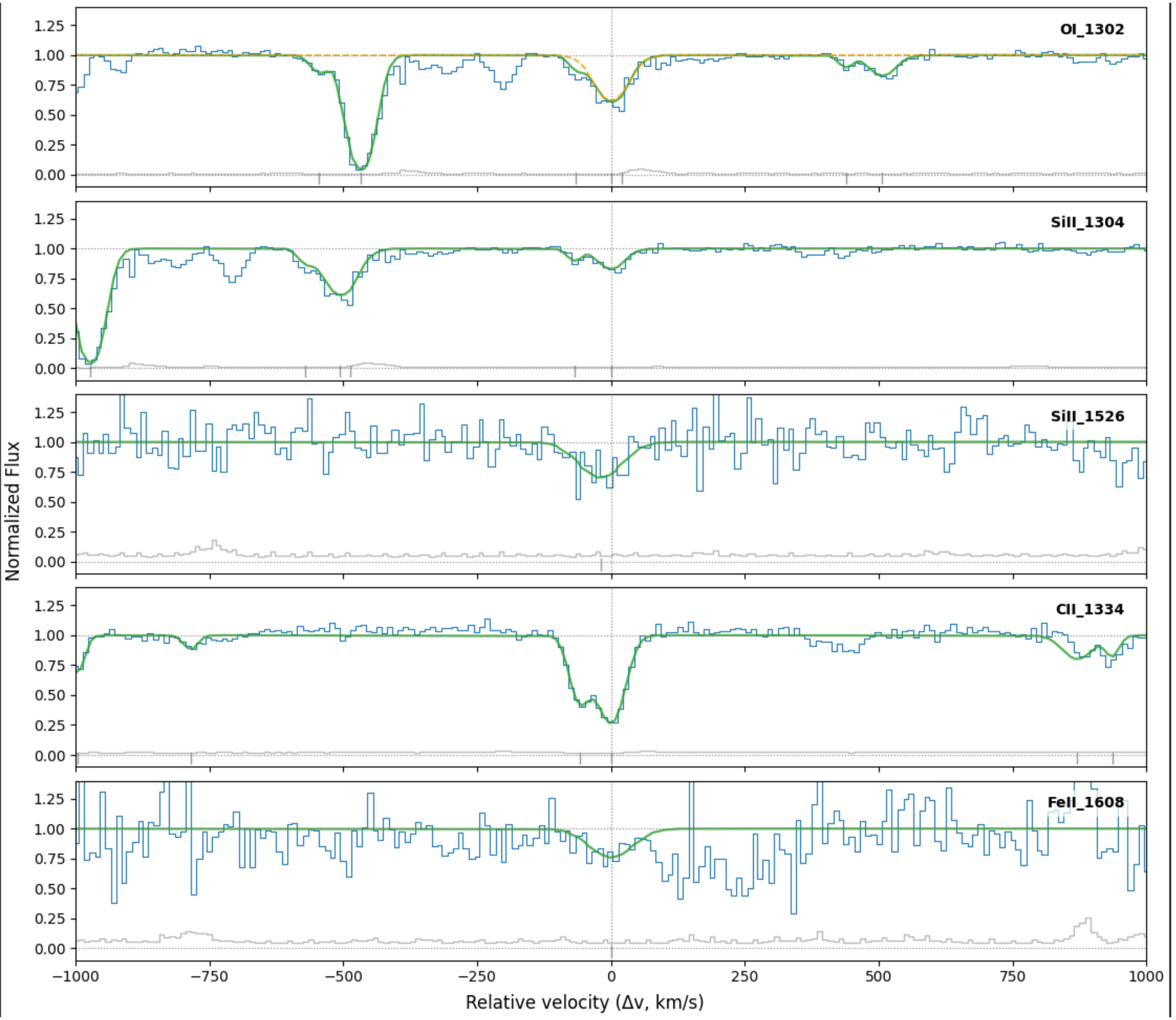

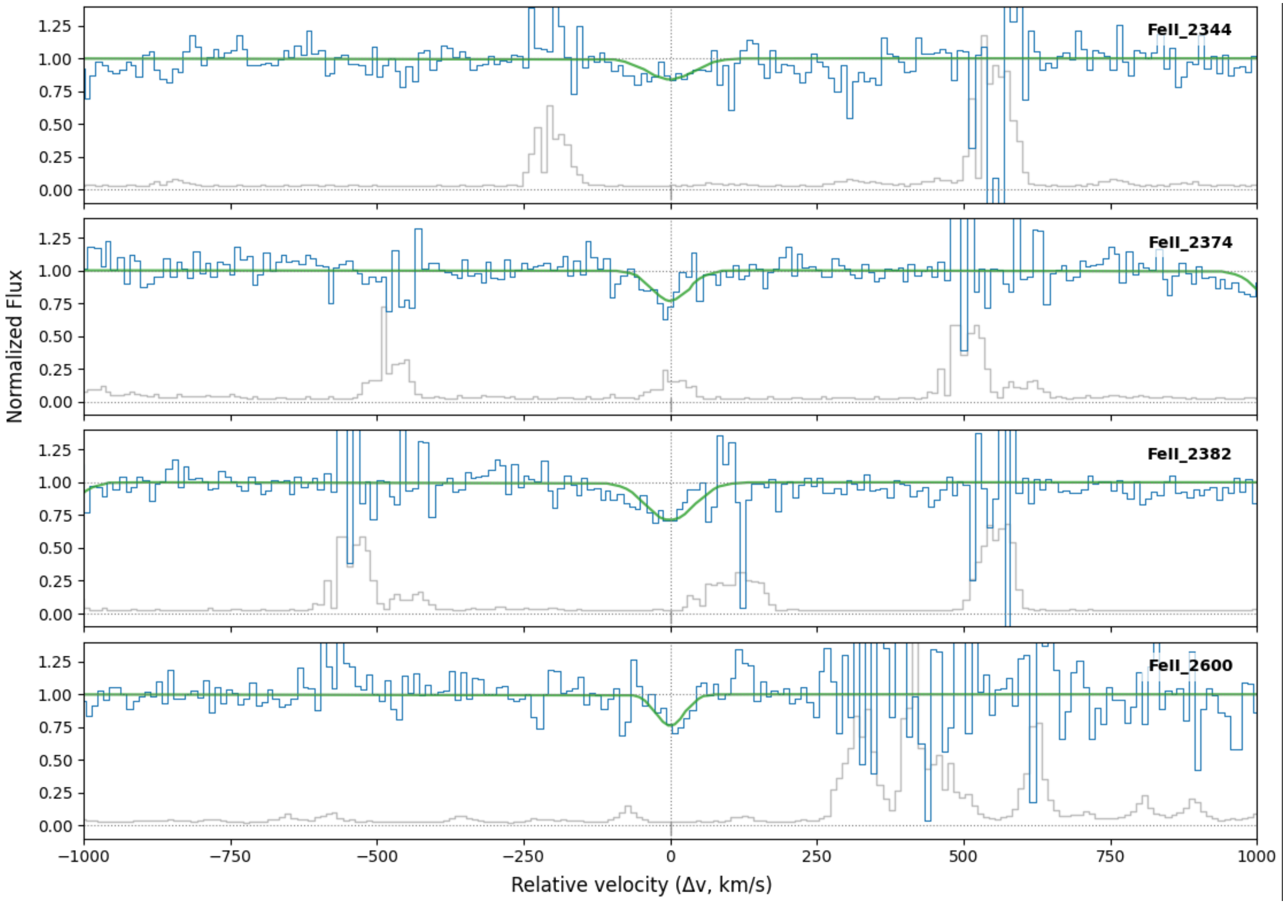

Intervening absorbers in J159-02 spectrum (1)

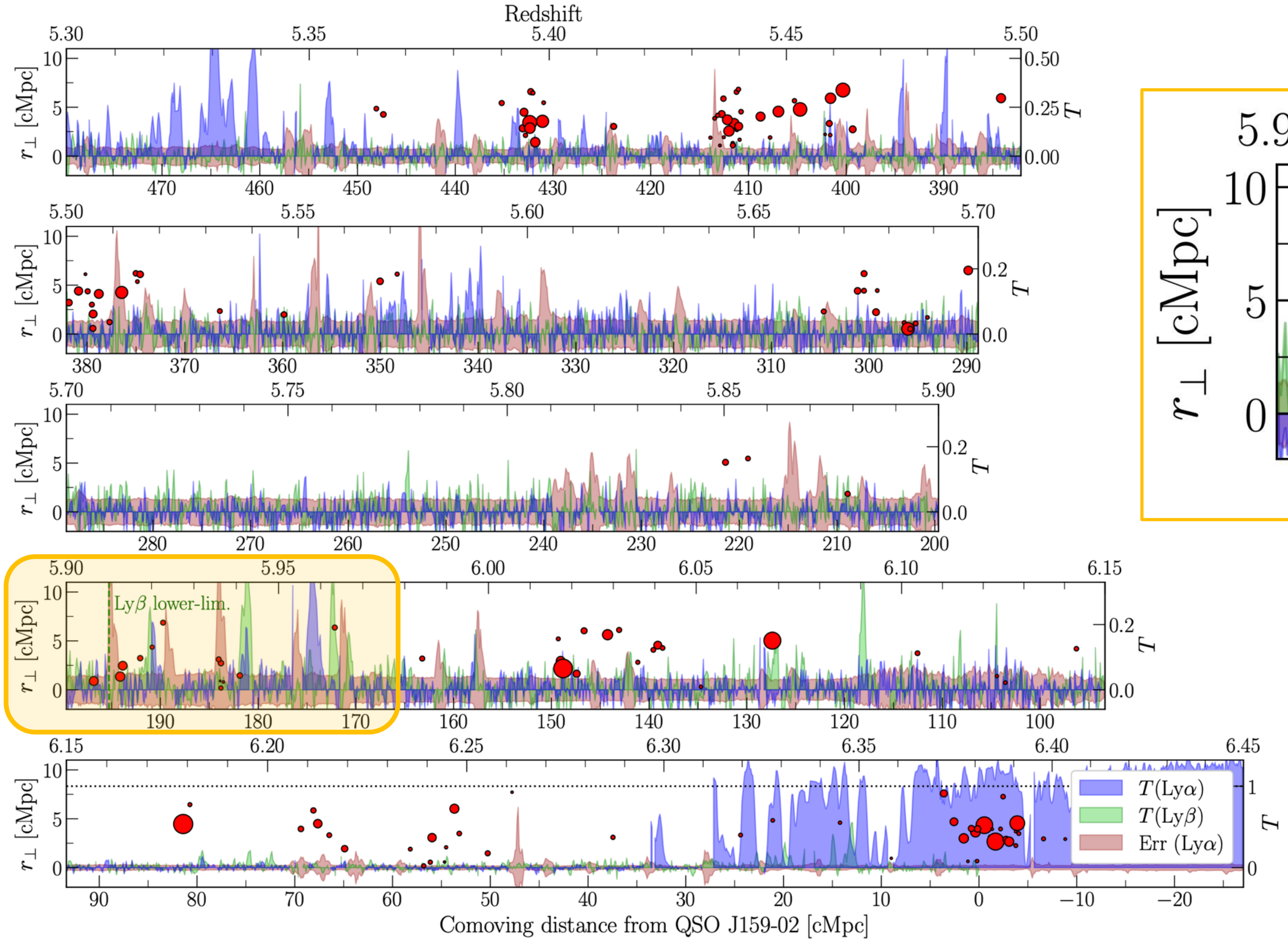

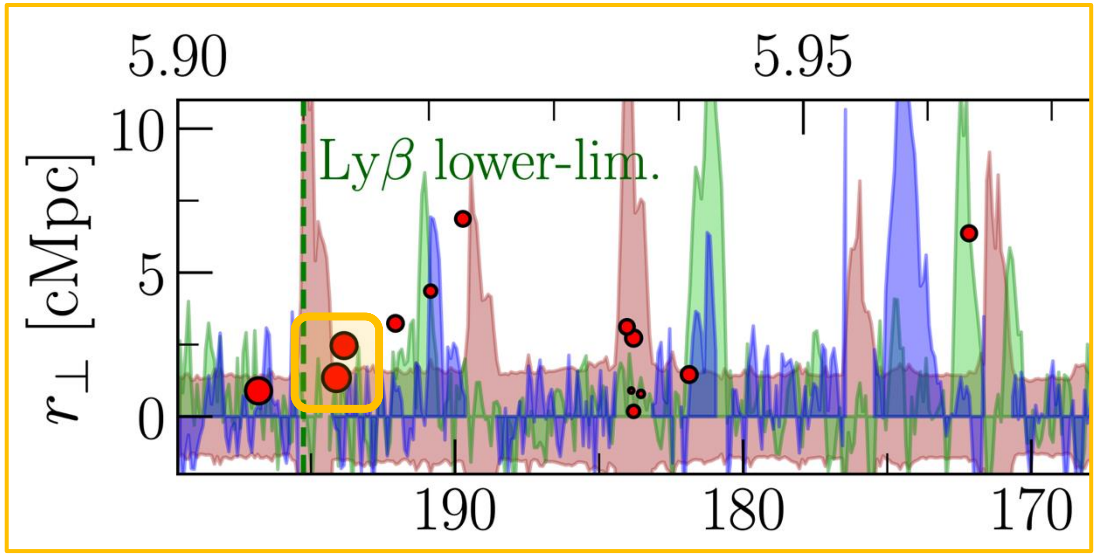

Kashino+ 2025

Intervening absorbers in J159-02 spectrum (2)

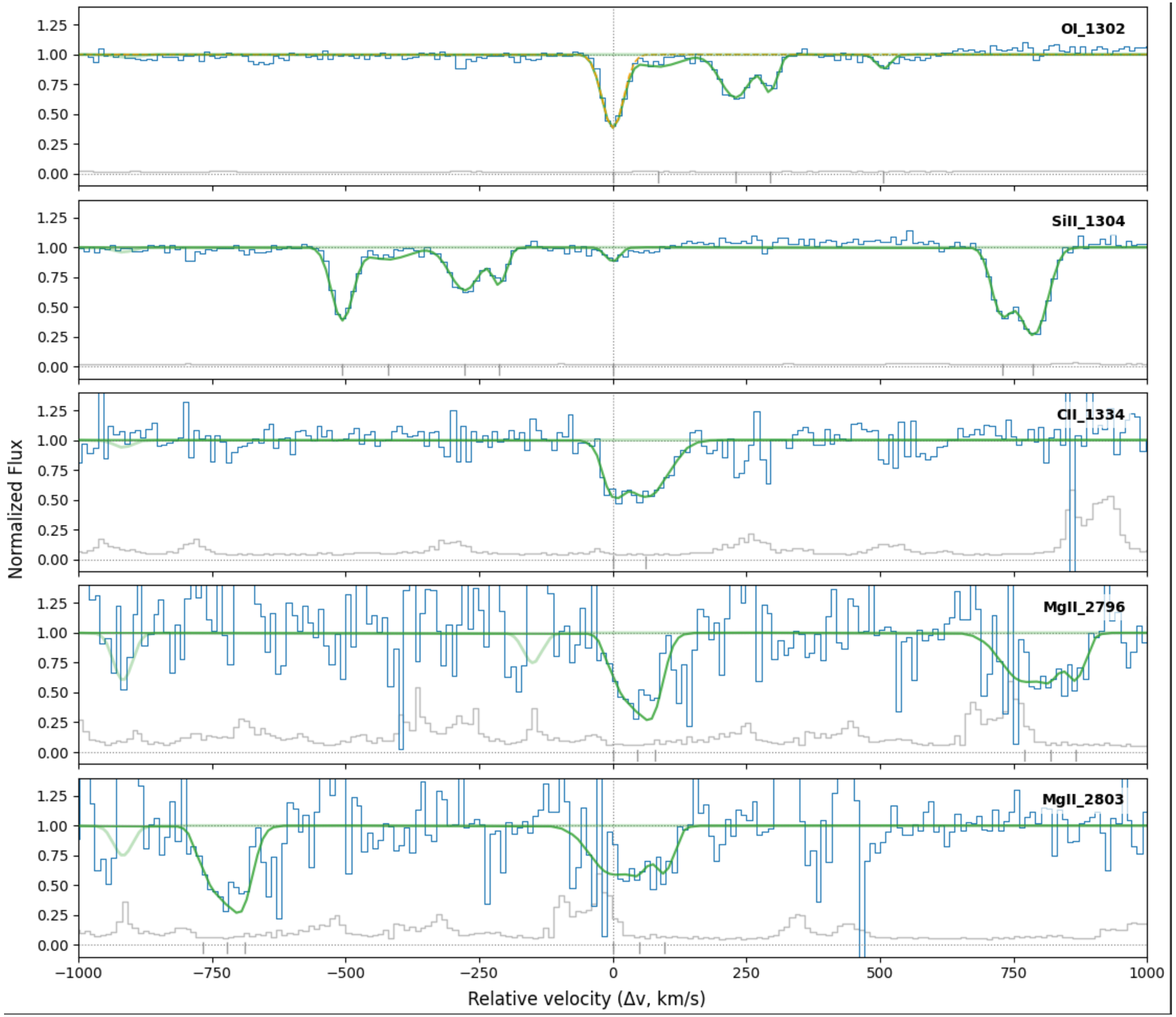

Absorption system at $z \sim 6.05443$

Kashino+ 2025

Intervening absorbers in J159-02 spectrum (2)

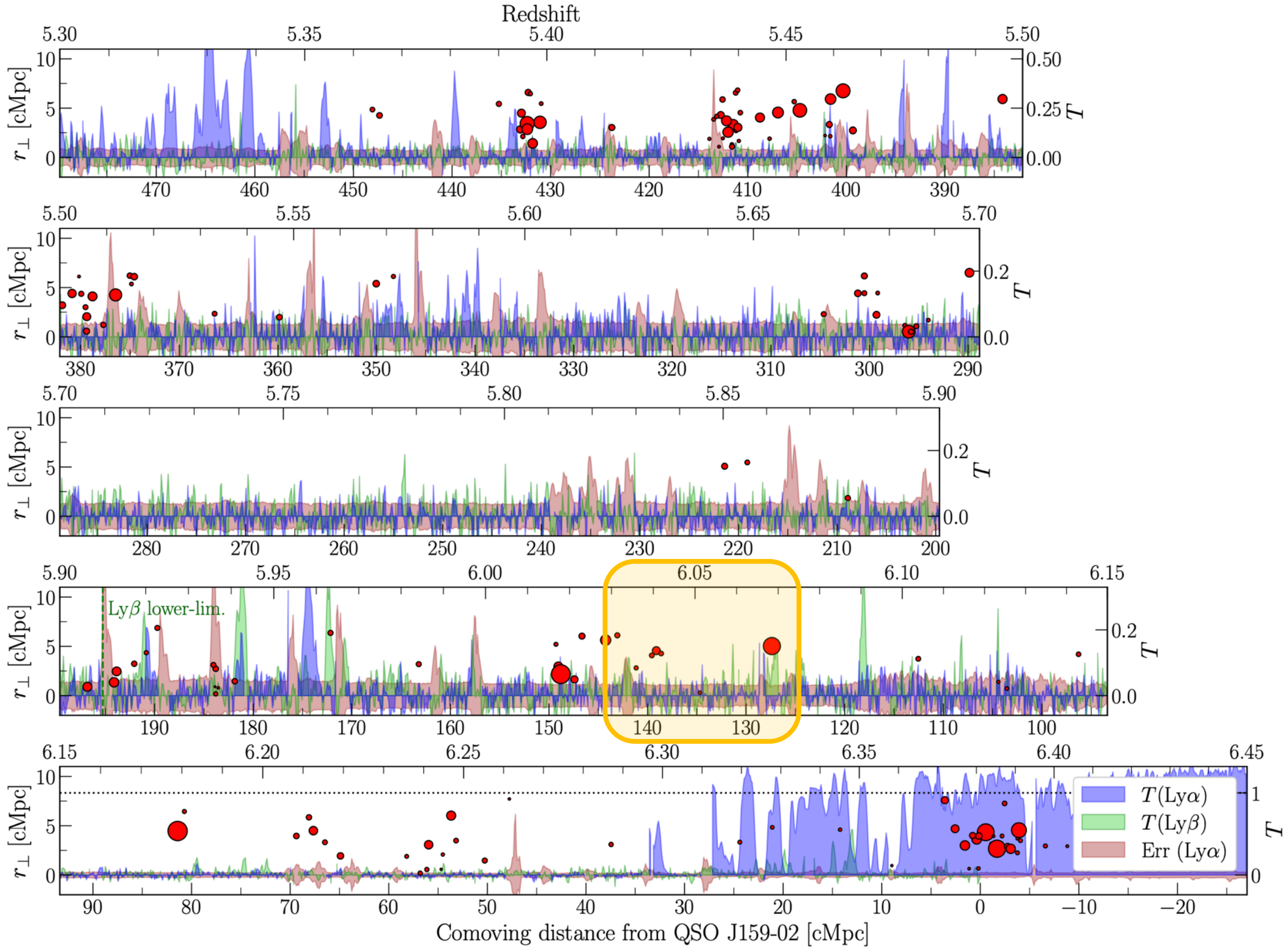

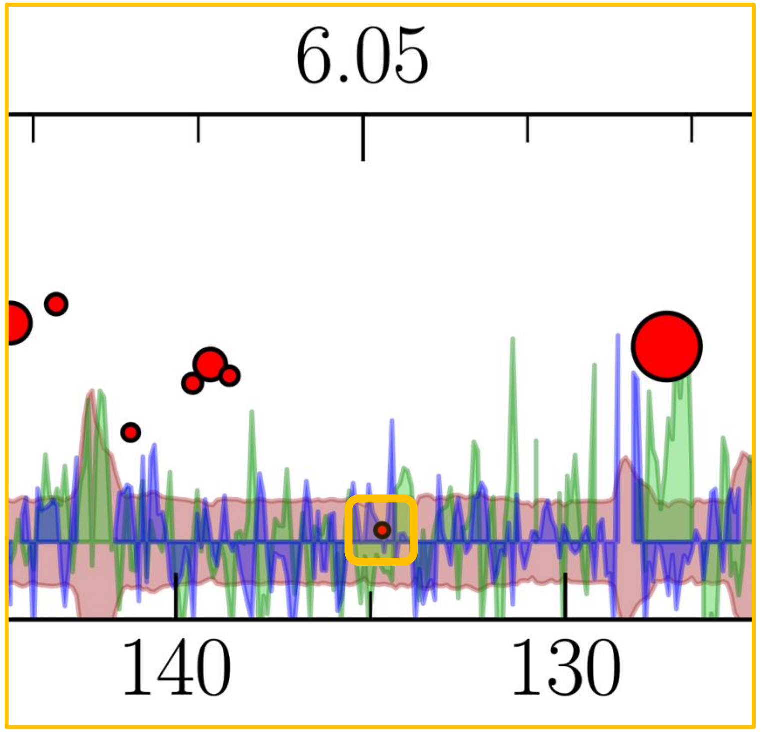

Kashino+ 2025

Intervening absorbers in J159-02 spectrum (3)

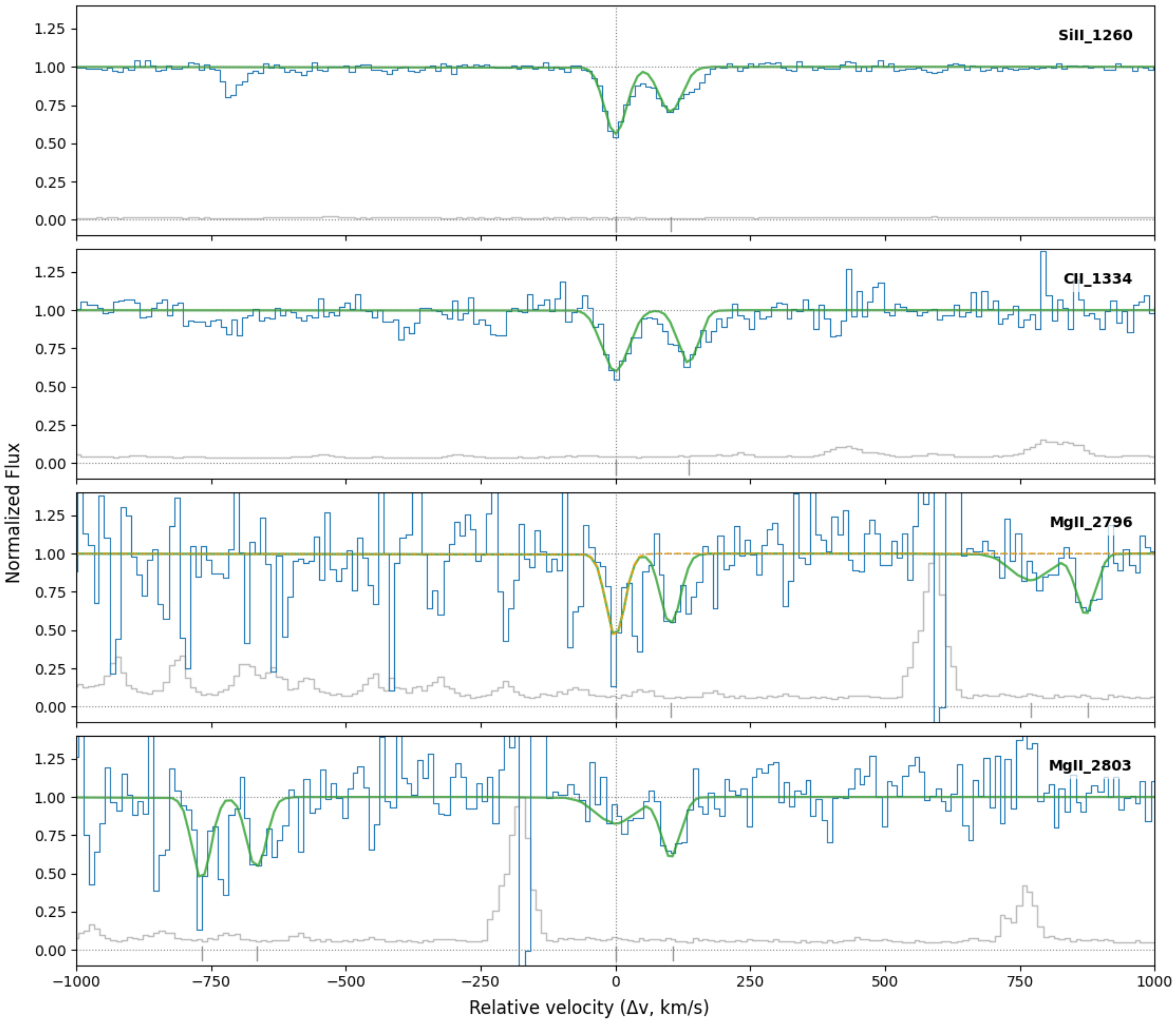

Absorption system at $z \sim 6.23694$

Kashino+ 2025

Intervening absorbers in J159-02 spectrum (3)

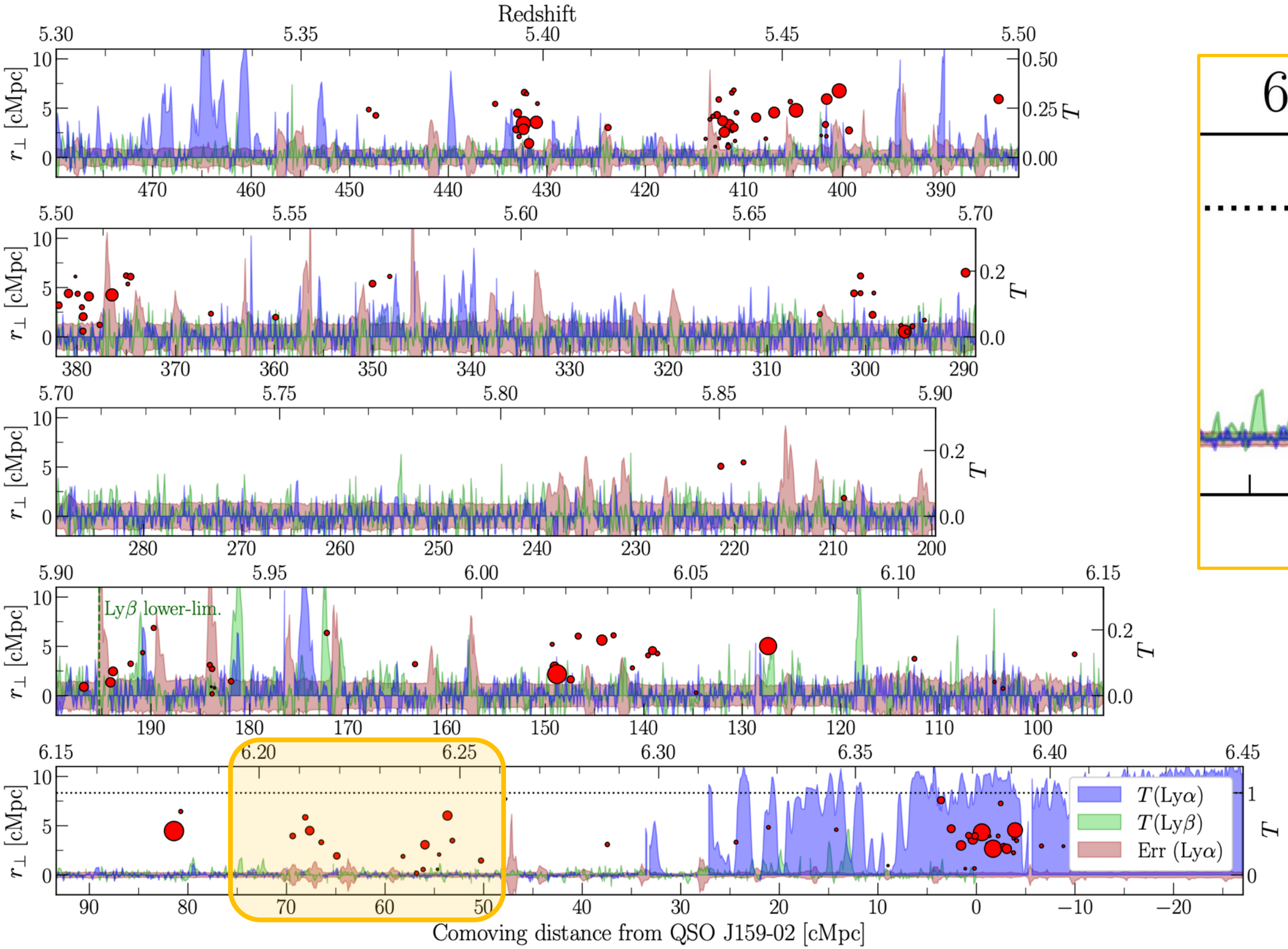

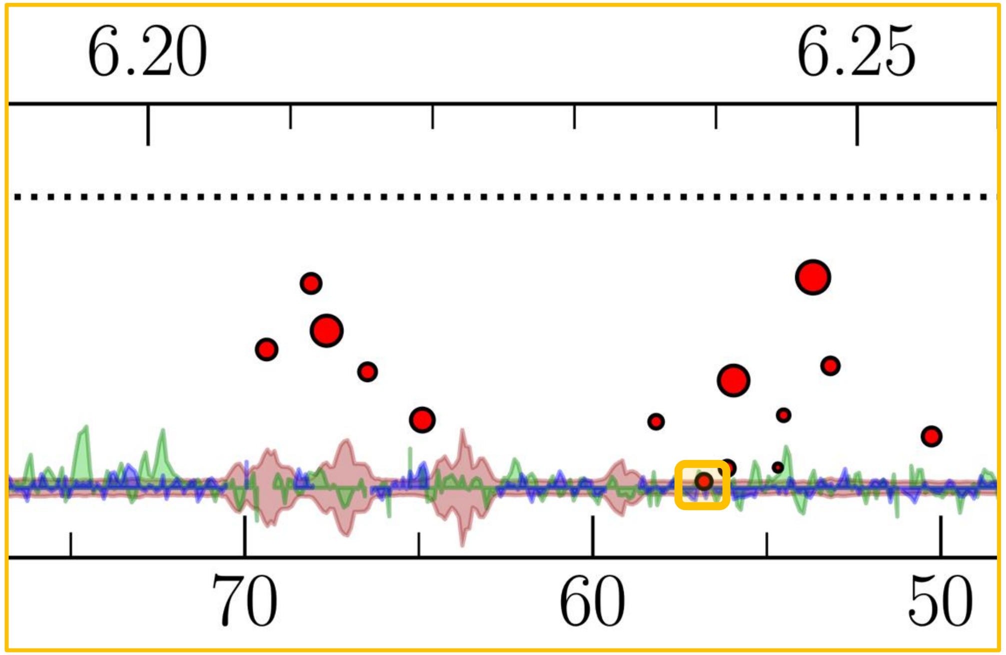

Kashino+ 2025

Intervening absorbers in J159-02 spectrum (4)

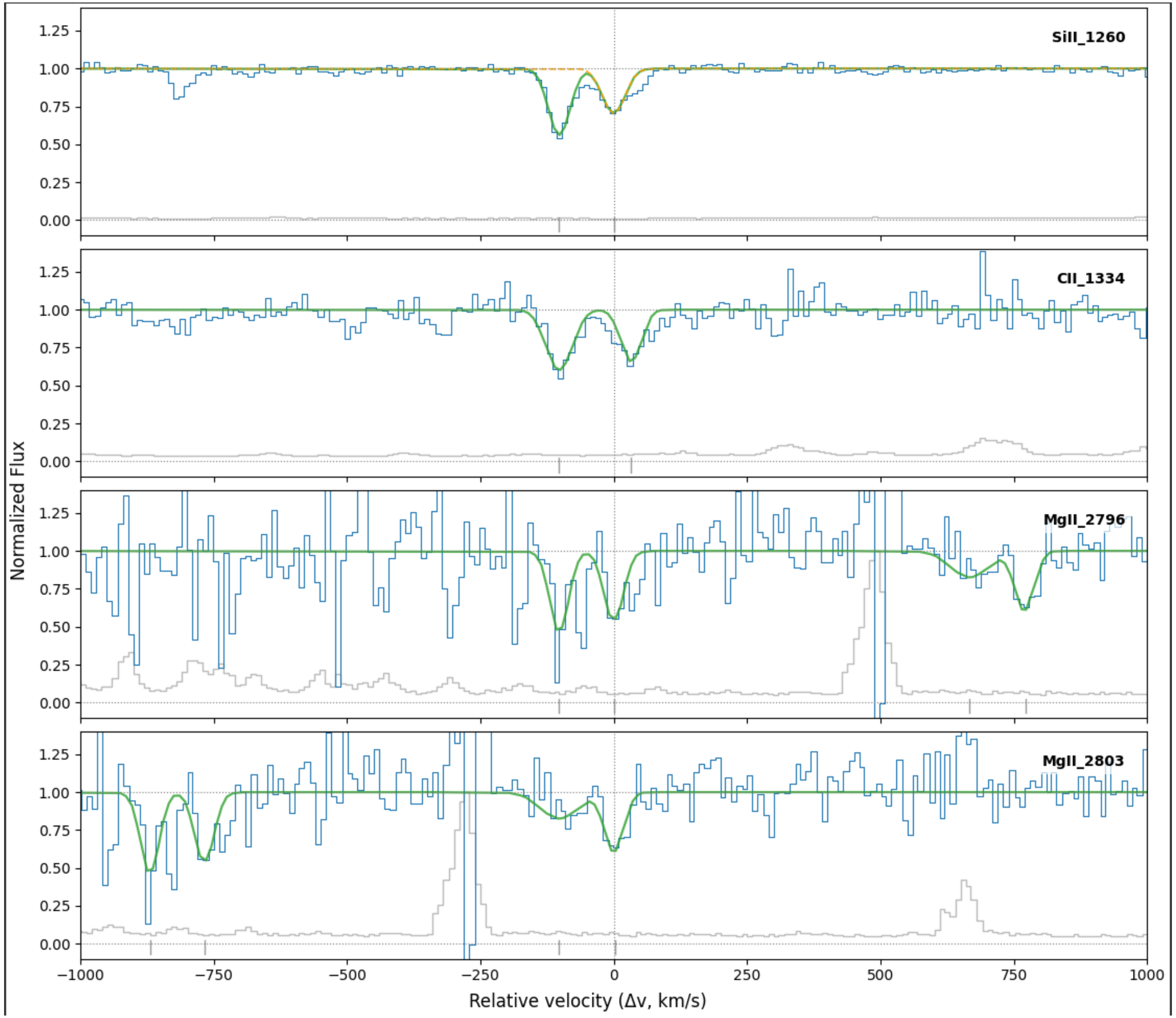

Absorption system at $z \sim 6.23941$

Intervening absorbers in J159-02 spectrum (4)

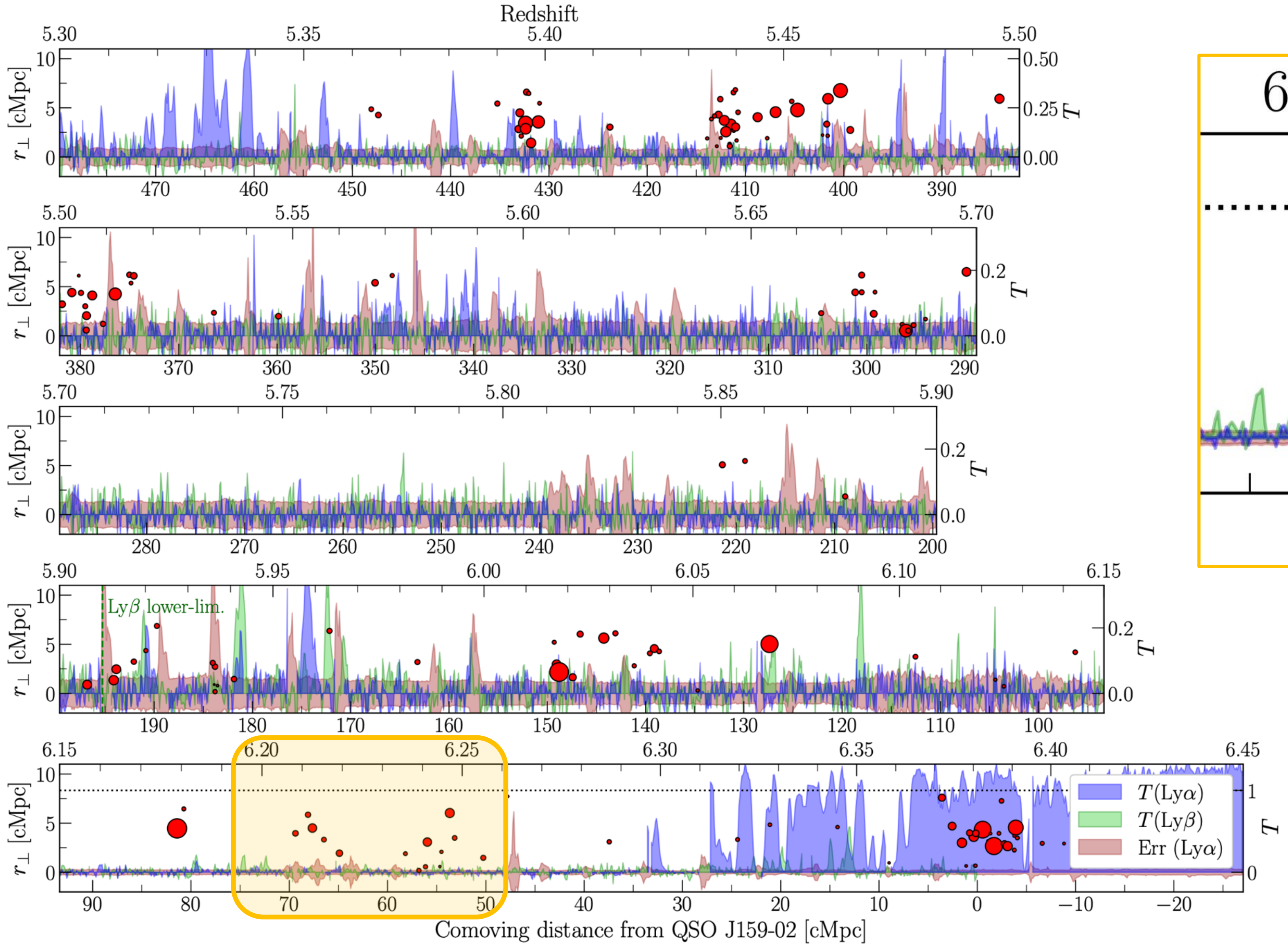

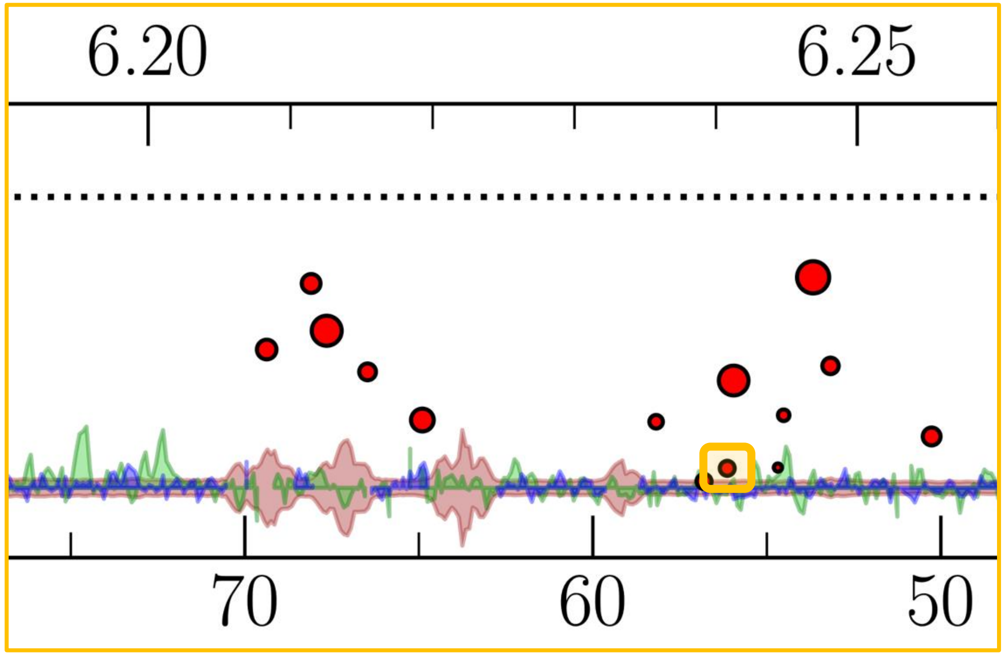

Kashino+ 2025

Intervening absorbers in J159-02 spectrum (5)

Absorption system at $z{\sim}5.73491$

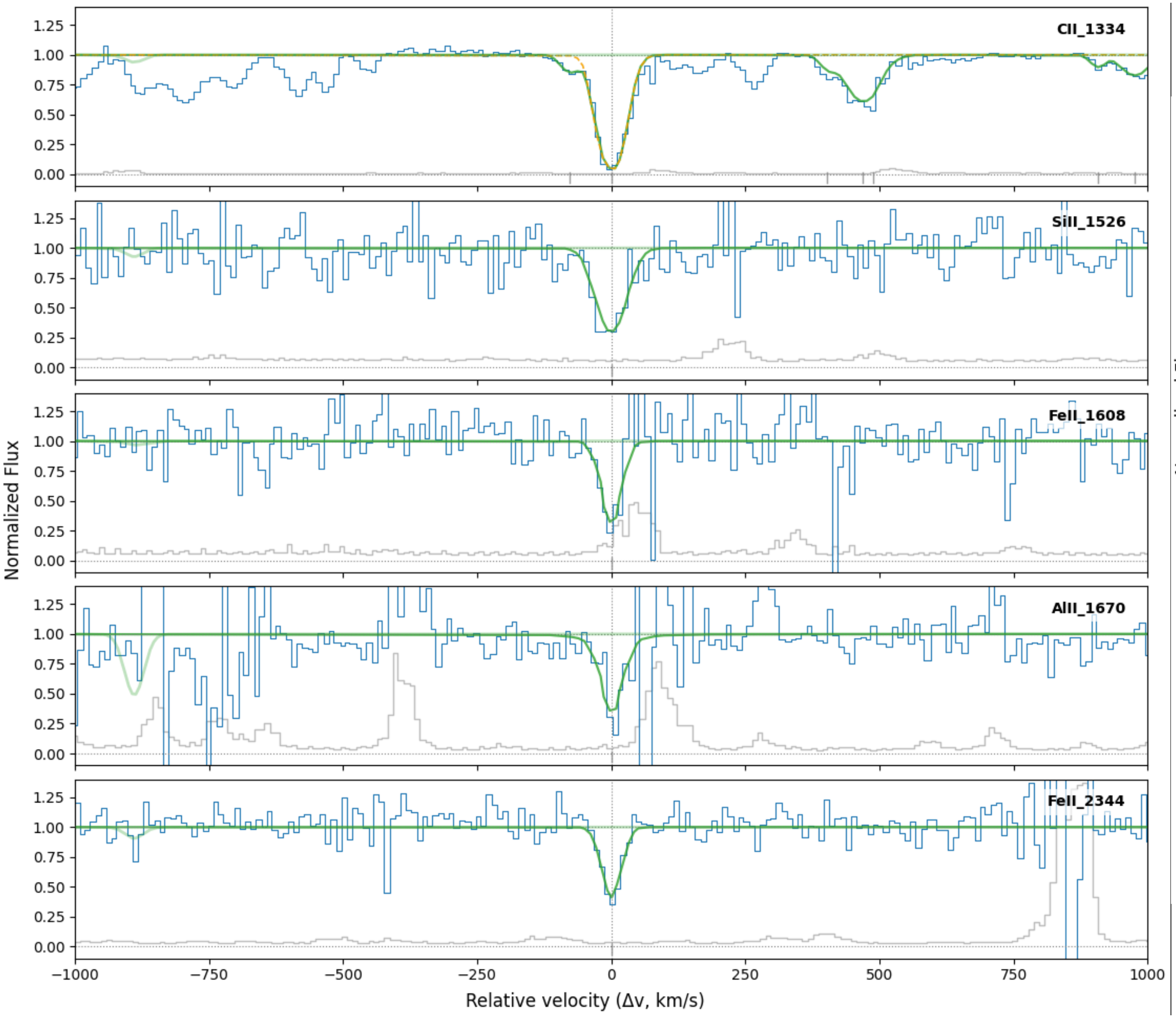

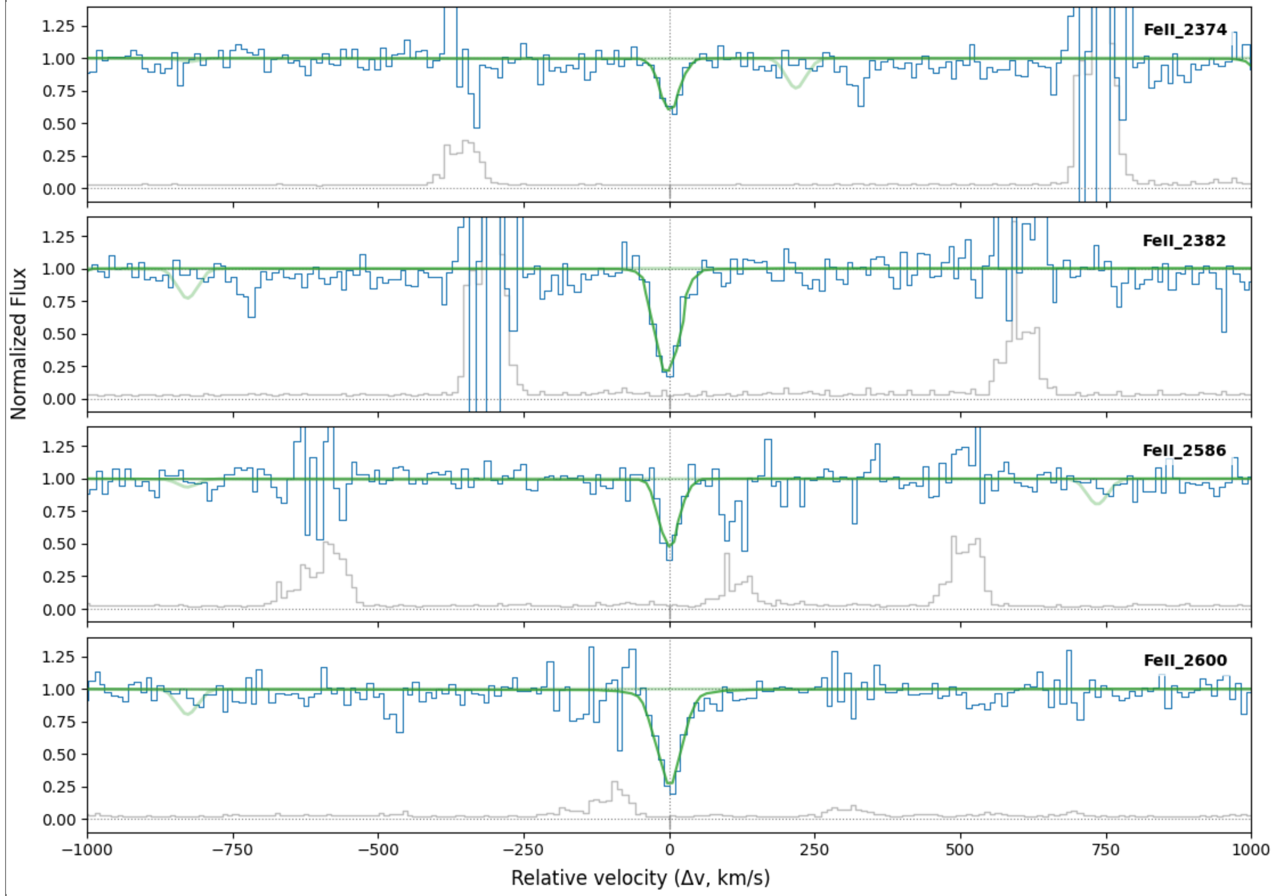

Intervening absorbers in J159-02 spectrum (5)

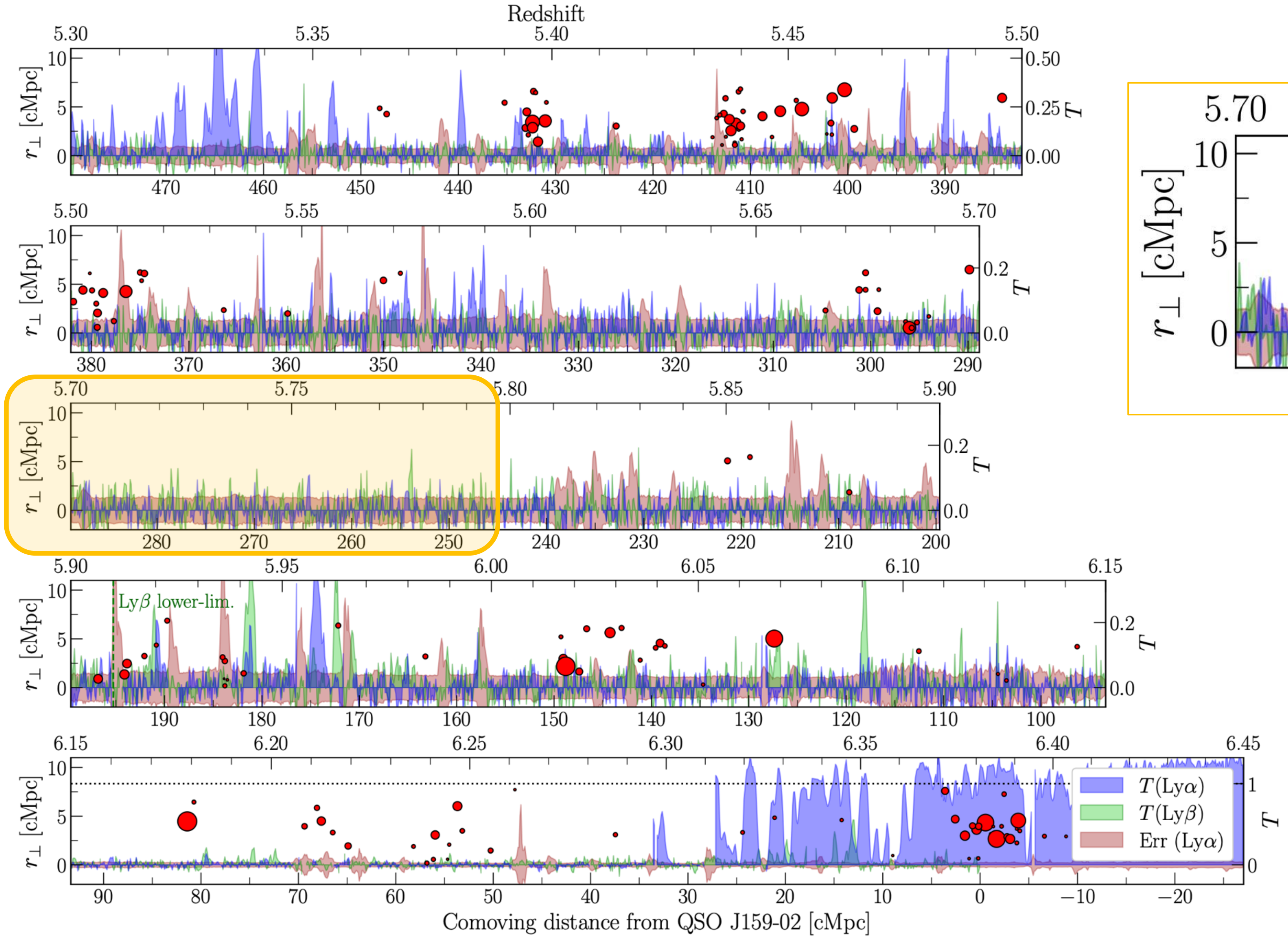

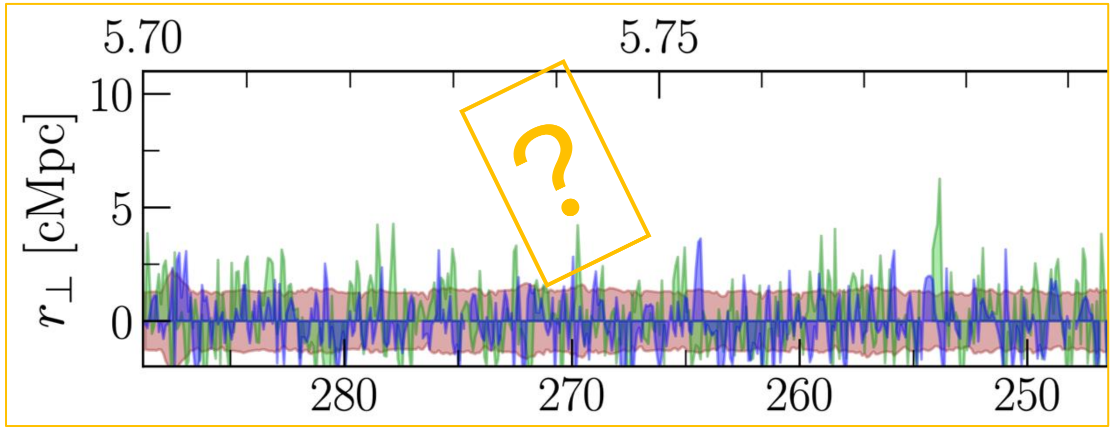

Low ionization absorption system without [O III] emitters counterpart!!!

Kashino+ 2025

Summary and Conclusion

- We reduced 2D raw spectroscopic data of the quasar PSOJ159-02 using ***PypeIt*** (Prochaska et al. 2020
- Fitted the continuum with power-law, Balmer continuum and iron emission
- Analysis of emission lines, with a focus on C IV and Mg II
- BH mass and λ_{Edd} estimate, comparing their values with literature
- Identifying absorption systems in the spectrum at different redshifts

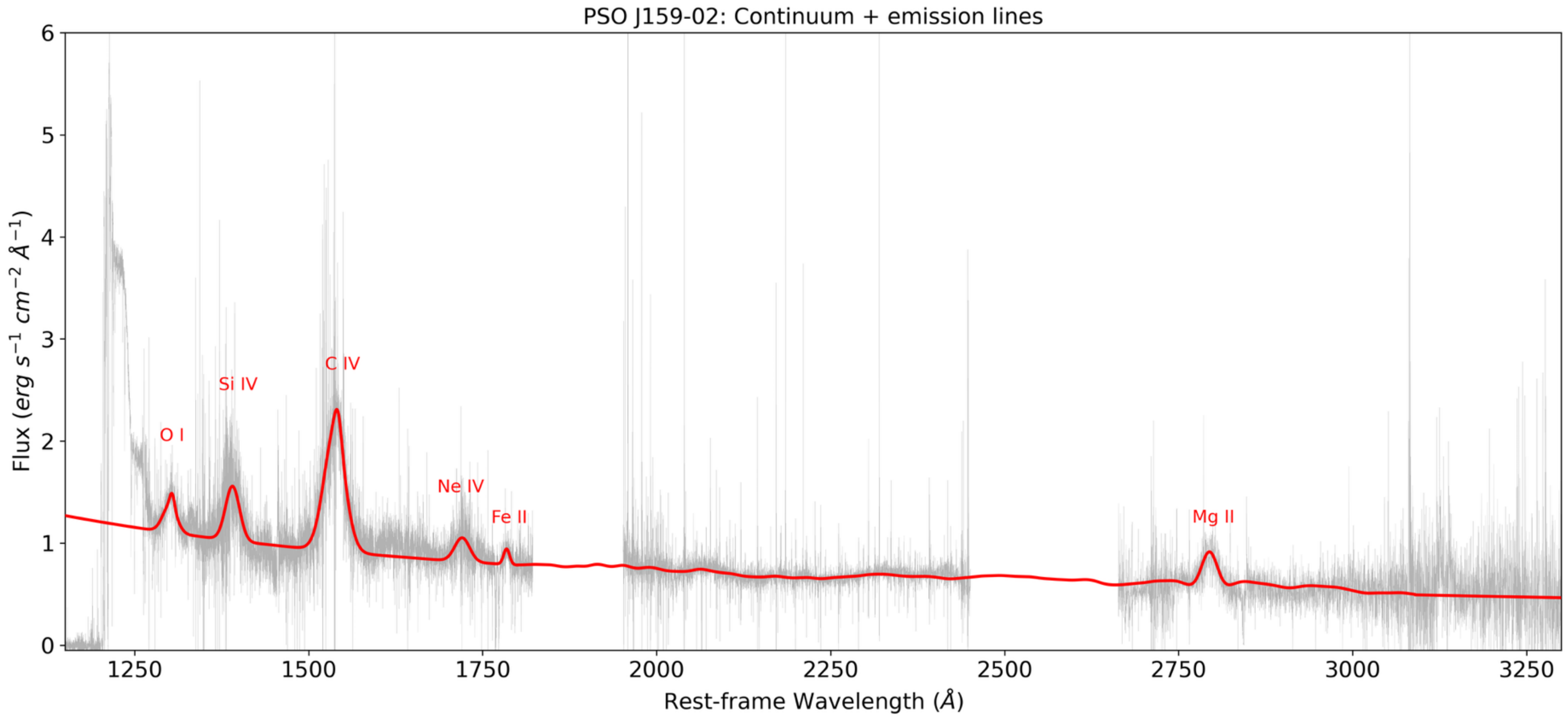

Data reduction (3)

The further steps consists of:

- **1D spectra coadding** and **stacking** of **multiple exposures**
  - Coadding routine construct wavelength grid which can be uniform in velocity. It has been chosen a dispersion of 10 km/s

- Fitting a **telluric absorption model** directly to the stacked quasar spectra **using** the telluric model grids produced from the Line-By-Line Radiative Transfer Model (***LBLRTM***: Clough et al. 2005)

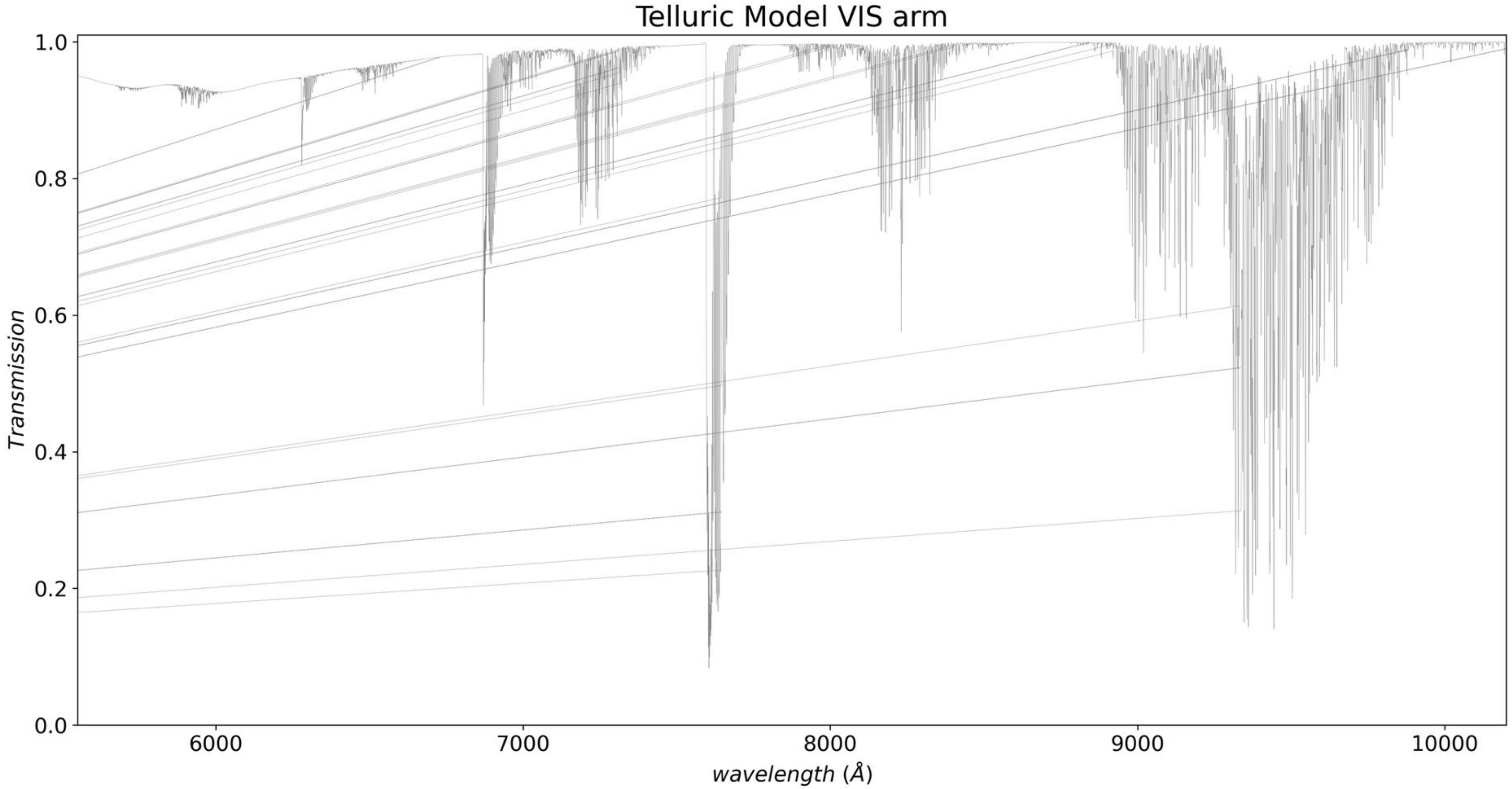

Data reduction (3)

The further steps consists of:

- **1D spectra coadding** and **stacking** of **multiple exposures**
  - Coadding routine construct wavelength grid which can be uniform in velocity. It has been chosen a dispersion of 10 km/s

- Fitting a **telluric absorption model** directly to the stacked quasar spectra **using** the telluric model grids produced from the Line-By-Line Radiative Transfer Model (***LBLRTM***: Clough et al. 2005)

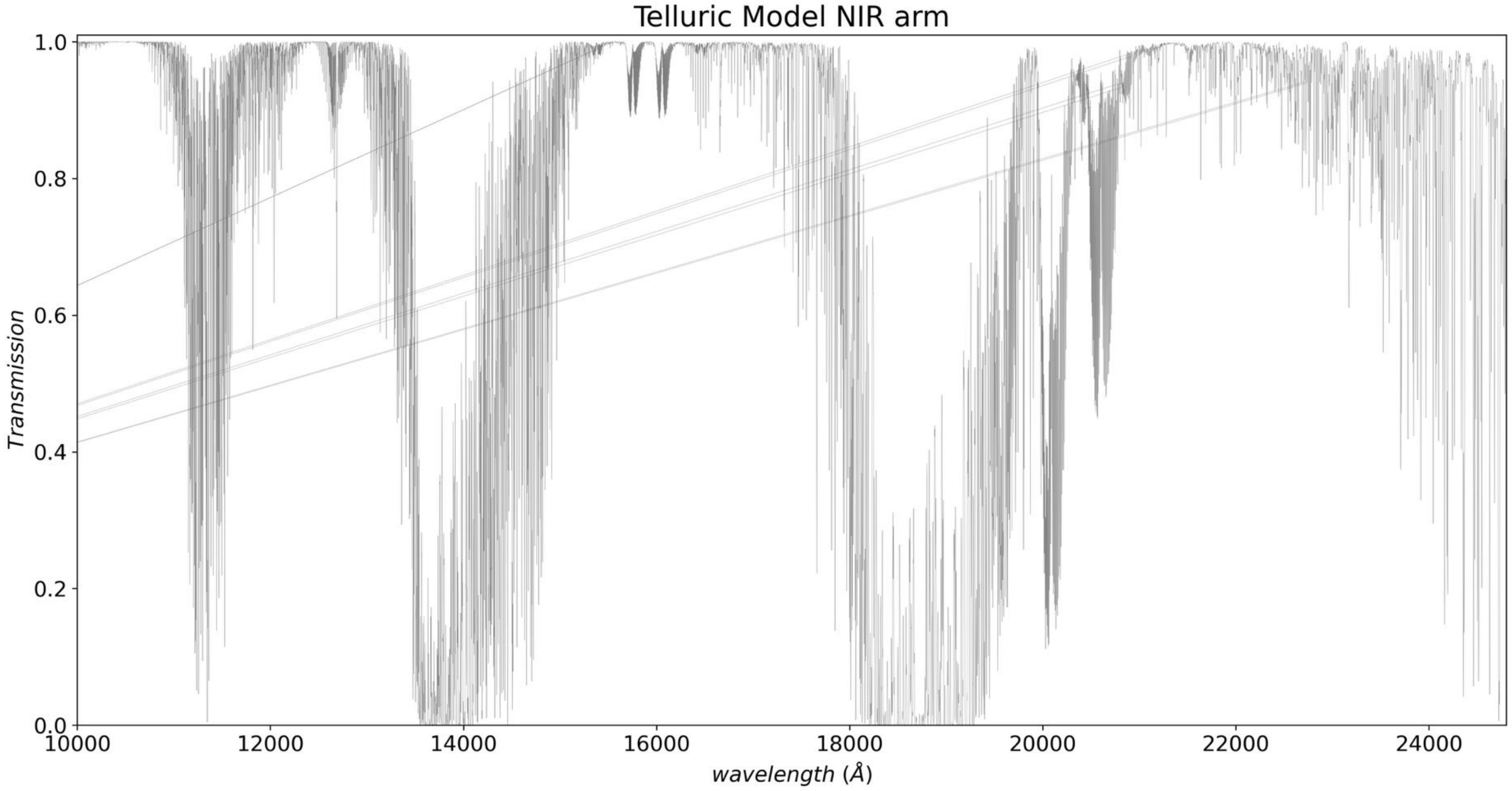

This work - Data reduction (2)

The further steps consists of:

- **Flux-calibration** of the individual 1-D spectrum **with the sensitivity function** derived from the standard star related to night observation

Star GD71 observed with VIS arm